

Palladium(II) and Platinum(II) Organometallic Complexes with the Model Nucleobase Anions of Thymine, Uracil, and Cytosine: Antitumor Activity and Interactions with DNA of the Platinum Compounds[○]

José Ruiz,^{*,†} Julia Lorenzo,[‡] Laura Sanglas,[‡] Natalia Cutillas,[†] Consuelo Vicente,[†] María Dolores Villa,[†] Francesc X. Avilés,[‡] Gregorio López,[†] Virtudes Moreno,[§] José Pérez,^{||} and Delia Bautista[⊥]

Departamento de Química Inorgánica, Universidad de Murcia, 30071-Murcia, Spain, Institut de Biotecnologia i Biomedicina, Department de Bioquímica i de Biologia Molecular, Universitat Autònoma de Barcelona, 08193 Barcelona, Spain, Department de Química Inorgànica, Universitat de Barcelona, Martí i Franquès 1-11, 08028 Barcelona, Spain, Departamento de Ingeniería Minera, Geológica y Cartográfica, Área de Química Inorgánica, Universidad Politécnica de Cartagena, 30203-Cartagena, Spain, and SUIC, Edificio SACE, Universidad de Murcia, 30071-Murcia, Spain

Received March 7, 2006

Pd(II) and Pt(II) complexes with the anions of the model nucleobases 1-methylthymine (1-MethyH), 1-methyluracil (1-MeuraH), and 1-methylcytosine (1-MecytH) of the types [Pd(dmba)(μ -L)]₂ [dmba = N,C-chelating 2-(dimethylamino)methylphenyl; L = 1-Methy, 1-Meura or 1-Mecyt] and [M(dmba)(L)(L')] [L = 1-Methy or 1-Meura; L' = PPh₃ (M = Pd or Pt), DMSO (M = Pt)] have been obtained. Palladium complexes of the types [Pd(C₆F₅)(N–N)(L)] [L = 1-Methy or 1-Meura; N–N = N,N,N',N'-tetramethylethylenediamine (tmeda), 2,2'-bipyridine (bpy), or 4,4'-dimethyl-2,2'-bipyridine (Me₂bpy)] and [NBu₄][Pd(C₆F₅)(1-Methy)₂(H₂O)] have also been prepared. The crystal structures of [Pd(dmba)(μ -1-Methy)]₂, [Pd(dmba)(μ -1-Mecyt)]₂·2CHCl₃, [Pd(dmba)(1-Methy)(PPh₃)₃]·3CHCl₃, [Pt(dmba)(1-Methy)(PPh₃)], [Pd(tmeda)(C₆F₅)(1-Methy)], and [NBu₄][Pd(C₆F₅)(1-Methy)₂(H₂O)]·H₂O have been established by X-ray diffraction. The DNA adduct formation of the new platinum complexes synthesized was followed by circular dichroism and electrophoretic mobility. Atomic force microscopy images of the modifications caused by the platinum complexes on plasmid DNA pBR322 were also obtained. Values of IC₅₀ were also calculated for the new platinum complexes against the tumor cell line HL-60. All the new platinum complexes were more active than cisplatin (up to 20-fold in some cases).

Introduction

The faster reaction kinetics of Pd(II) electrophiles as compared to the corresponding Pt(II) compounds (ca. 10⁵ times) yet otherwise similar chemistry of the two metals make the former convenient analogues for studies of Pt–nucleobase interactions.^{1–4} Studies of this kind are of interest

with respect to the mode of action of Pt antitumor drugs.⁵ Pyrimidine nucleobases (Scheme 1), particularly in their anionic forms, are versatile ligands. In fact, their several potential donor sites enable them to form homo- and heteropolynuclear complexes. These compounds can exhibit metal–metal interactions which nature have been examined.^{6–8} Few studies have been directed toward organometallic

* To whom correspondence should be addressed. E-mail: jruiz@um.es. Fax: (+34) 968 36 41 48.

[†] Departamento de Química Inorgánica, Universidad de Murcia.

[‡] Institut de Biotecnologia i Biomedicina, Universitat Autònoma de Barcelona.

[§] Department de Química Inorgànica, Universitat de Barcelona.

^{||} Área de Química Inorgánica, Universidad Politécnica de Cartagena.

[⊥] Edificio SACE, Universidad de Murcia.

[○] Dedicated to Dr. José-Antonio Abad on the occasion of his retirement.

(1) Micklitz, W.; Sheldrick, W. S.; Lippert, B. *Inorg. Chem.* **1990**, *29*, 211.

(2) Barnham, K. J.; Bauer, C. J.; Djuran, M. I.; Mazid, M. A.; Rau, T.; Sadler, P. J. *Inorg. Chem.* **1995**, *34*, 2826.

(3) Shen, W.-Z.; Gupta, D.; Lippert, B. *Inorg. Chem.* **2005**, *44*, 8249.

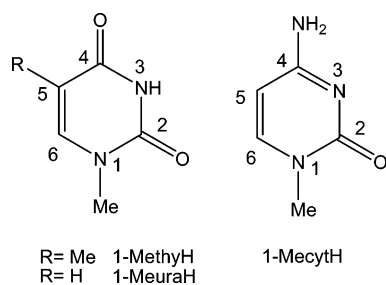
(4) *Cisplatin. Chemistry and Biochemistry of a leading Anticancer Drug*; Lippert, B., Ed.; Wiley-VCH: Weinheim, Germany, 1999.

(5) Jamieson, E. R.; Lippard, S. J. *Chem. Rev.* **1999**, *99*, 2467.

(6) Mealli, C.; Pichierri, F.; Randaccio, L.; Zangrando, E.; Krumm, M.; Holthenrich, D.; Lippert, B. *Inorg. Chem.* **1995**, *34*, 3418.

(7) Kampf, G.; Willermann, M.; Freisinger, E.; Lippert, B. *Inorg. Chim. Acta* **2002**, *330*, 179.

Scheme 1



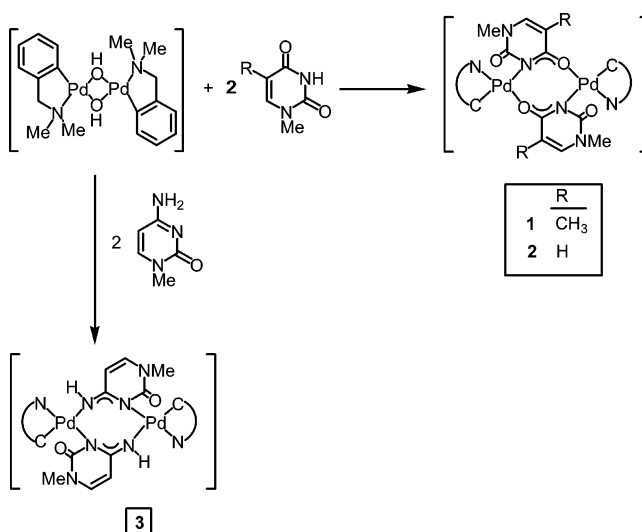
complexes with these biologically important ligands,^{9,10} organometallic complexes with bioligands representing new directions for structural diversity, possible new drug discoveries, and the ability of these complexes to be hosts for biologically important guests.⁹

The aim of this work is the synthesis of new palladium and platinum complexes having the metal covalently bonded to the nucleobase which can be used in biological experiments as potential anticancer drugs or as metalated nucleobase building blocks that can be incorporated into synthetic oligonucleotides. Oligonucleotides metalated at fixed positions could possess improved and site-specific biological activity. Nephrotoxic side effects associated with therapies based on metal complexes, caused by the excess of metal used and by their uncontrolled biodistribution, can be reduced by linking the metal to specific biological targets such as oligonucleotides.^{11–13} Therefore, even today, the synthesis of metallonucleosides is still very interesting.

On the other hand, the hydroxo complexes $[\text{Pd}(\text{dmba})(\mu\text{-OH})_2]$ (dmba = *N,C*-chelating 2-((dimethylamino)methyl)phenyl)¹⁴ and $[\text{Pd}(\text{C}_6\text{F}_5)(\text{N}-\text{N})(\text{OH})]$ (*N-N* = bpy, Me_2bpy , or tmeda with bpy = 2,2'-bipyridine, Me_2bpy = 4,4'-dimethyl-2,2'-bipyridine, tmeda = *N,N,N',N'*-tetramethylethylenediamine)¹⁵ have shown to be excellent precursors in organometallic synthesis.^{14–19}

We report here the synthesis and characterization of new organopalladium and organoplatinum complexes with the model nucleobase anions of 1-methyluracil (1-MeuraH), 1-methylthymine (1-MethyH), and methylcytosine (1-

Scheme 2



MecytH) (Scheme 1) of the types $[\text{Pd}(\text{dmba})(\mu\text{-L})_2]$ (*L* = 1-Methy, 1-Meura, or 1-Mecyt), $[\text{M}(\text{dmba})(\text{L})(\text{L}')]]$ [*L* = 1-Methy or 1-Meura; *L'* = PPh_3 (*M* = Pd or Pt), DMSO (*M* = Pt)], $[\text{Pd}(\text{C}_6\text{F}_5)(\text{N}-\text{N})(\text{L})]$ [*L* = 1-Methy or 1-Meura; *N-N* = tmeda, bpy, or Me_2bpy], and $[\text{NBu}_4][\text{Pd}(\text{C}_6\text{F}_5)(1\text{-Methy})_2(\text{H}_2\text{O})]$. We also report the crystal structures of some of these palladium or platinum complexes. To our knowledge, the structures of complexes $[\text{Pd}(\text{dmba})(\mu\text{-L})_2]$ (*L* = 1-Methy, 1-Mecyt) represent the first examples of Pd(II) organometallic complexes with two anionic pyrimidine nucleobases acting as bridging ligands being fully characterized by X-ray diffraction and the structure of $[\text{NBu}_4][\text{Pd}(\text{C}_6\text{F}_5)(1\text{-Methy})_2(\text{H}_2\text{O})]\cdot\text{H}_2\text{O}$ is the first crystal structure of a monomeric palladium bis(thyminate) complex.

We have also studied the interactions of the platinum complexes with DNA by circular dichroism and electrophoretic mobility. Atomic force microscopy images of the modifications caused by the platinum complexes on plasmid DNA pBR322 were also obtained. The *in vitro* antiproliferative activity of the new platinum complexes in HL-60 cell line has been studied.

Results and Discussion

Dimeric Palladium Complexes $[\text{Pd}(\text{dmba})(\mu\text{-L})_2]$ (*L* = 1-Methy, 1-Meura, 1-Mecyt). The reaction of the hydroxo-palladium complex¹⁴ $[\text{Pd}(\text{dmba})(\mu\text{-OH})_2]$ in dichloromethane with 1-methylthymine, 1-methyluracil, or 1-methylcytosine (in a 1:2 ratio) leads to the formation of the *N*(3),*O*-bridged (1-methylthyminato)- or (1-methyluracilato)dipalladium complexes $[\text{Pd}(\text{dmba})(\mu\text{-L})_2]$ [*L* = 1-Methy (**1**), 1-Meura (**2**)] or the *N*(3),*N*(4)-bridged (1-methylcytosinato)dipalladium complex (**3**) (Scheme 2). These reactions imply proton abstraction from the pyrimidine nucleobase by the hydroxo complex with the concomitant release of water. On protonation of the hydroxo complex, it is likely that an intermediate aqua complex is formed. As far as we know, complexes **1** and **2** represent the first examples of organometallic dinuclear palladium(II) complexes with 1-Methy⁻ or 1-Meura⁻ nucleobases. The analytical data are consistent

- (8) Ito, K.; Somozawa, R.; Matsunami, J.; Matsumoto, K. *Inorg. Chim. Acta* **2002**, *339*, 292.
- (9) Fish, R. H.; Jaouen, G. *Organometallics* **2003**, *22*, 2166.
- (10) Romanelli, A.; Iacovino, R.; Piccialli, G.; Rufo, F.; De Napoli, L.; Pedone, C.; Di Blasco, B.; Messere, A. *Organometallics* **2005**, *24*, 3401.
- (11) Navarro, J. A. R.; Romero, M. A.; Vilaplana, R.; González-Vilchez, F.; Faure, R. *J. Med. Chem.* **1988**, *31*, 332.
- (12) Pérez, J. M.; López-Solera, I.; Montero, E. I.; Brana, M. F.; Alonso, C.; Robinson, S. P.; Navarro-Ranninger, C. *J. Med. Chem.* **1999**, *42*, 5482.
- (13) Bierbach, U.; Sabat, M.; Farrell, N. *Inorg. Chem.* **2000**, *39*, 1882.
- (14) Ruiz, J.; Cutillas, N.; Rodríguez, V.; Sampedro, J.; López, G.; Chaloner, P. A.; Hitchcock, P. *J. Chem. Soc., Dalton Trans.* **1999**, 2939.
- (15) Ruiz, J.; Martínez, M. T.; Florenciano, F.; Rodríguez, V.; López, G.; Pérez, J.; Chaloner, P. A.; Hitchcock, P. B. *Inorg. Chem.* **2003**, *42*, 3650.
- (16) Ruiz, J.; Rodríguez, V.; Cutillas, N.; Pardo, M.; Pérez, J.; López, G.; Chaloner, P. A.; Hitchcock, P. B. *Organometallics* **2001**, *20*, 1973.
- (17) Ruiz, J.; Martínez, M. T.; Florenciano, F.; Rodríguez, V.; López, G.; Pérez, J.; Chaloner, P. A.; Hitchcock, P. B. *Dalton Trans.* **2004**, 929.
- (18) Ruiz, J.; Martínez, M. T.; Rodríguez, V.; López, G.; Pérez, J.; Chaloner, P. A.; Hitchcock, P. B. *Dalton Trans.* **2004**, 3521.
- (19) Ruiz, J.; Vicente, C.; Cutillas, N.; Pérez, J. *Dalton Trans.* **2005**, 1999.

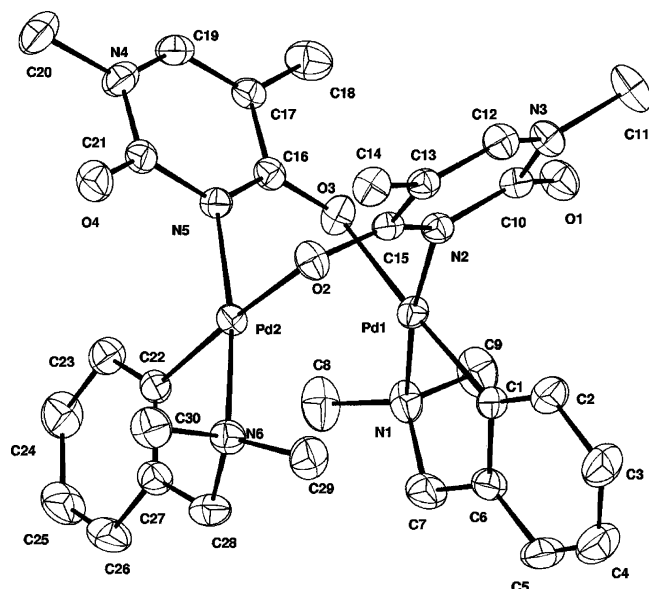


Figure 1. ORTEP of complex **1**, showing the atom-numbering scheme. Displacement ellipsoids are drawn at the 50% probability level.

Table 1. Selected Distances (Å) and Bond Angles (deg) for Complex **1**

Bond Distances		Bond Angles	
Pd(1)–C(1)	1.970(3)	C(1)–Pd(1)–N(2)	91.58(11)
Pd(1)–N(2)	2.068(2)	C(1)–Pd(1)–N(1)	82.81(12)
Pd(1)–N(1)	2.095(2)	N(2)–Pd(1)–N(1)	172.36(10)
Pd(1)–O(3)	2.150(2)	C(1)–Pd(1)–O(3)	172.01(11)
Pd(2)–C(22)	1.967(3)	N(2)–Pd(1)–O(3)	92.85(9)
Pd(2)–N(5)	2.056(2)	N(1)–Pd(1)–O(3)	92.15(10)
Pd(2)–N(6)	2.074(3)	C(22)–Pd(2)–N(5)	93.64(11)
Pd(2)–O(2)	2.133(2)	C(22)–Pd(2)–N(6)	82.76(12)
Pd(1)···Pd(2)	3.008(1)	N(5)–Pd(2)–N(6)	171.47(10)
		C(22)–Pd(2)–O(2)	172.82(11)
		N(5)–Pd(2)–O(2)	93.18(9)
		N(6)–Pd(2)–O(2)	90.17(10)

with the proposed formulas. The FAB mass spectra show peaks at $m/z = 760$ (for **1**), 732 (for **2**), and 730 ($M - \text{CH}_2\text{Cl}_2$)⁺ for **3** confirming the dimeric nature of these complexes. The IR of **1** shows an intense mode for 1-Methy at ca. 1540 cm^{-1} which indicates strong metal binding to both N(3) and the exocyclic oxygen O(4). The other intense IR band in the double-bond stretching region, at ca. 1640 cm^{-1} , is frequently split in 1-Methy compounds ($\Delta = 15 \text{ cm}^{-1}$).¹

Crystal Structures of 1 and 3·2CHCl₃. Figure 1 shows the X-ray structure of complex **1**, with selected bond lengths and angles listed in Table 1. To our knowledge, this compound represents the first example of an organometallic palladium(II) complex with two 1-methylthyminato nucleobases acting as bridges being fully characterized by X-ray diffraction.²⁰ The complex consists of two $\{(o\text{-C}_6\text{H}_4\text{CH}_2\text{-NMe}_2)\text{Pd}\}$ fragments each bridged by two 1-methylthyminato ligands through N(3) and O(4) with a head-to-tail arrangement and anti structure. The intramolecular Pd···Pd distance in complex **1** is $3.008(1) \text{ Å}$, a bit longer than the shortest value found so far (2.861 Å) for a head-to-tail 1-methylthyminato-bridged palladium complex which has been observed in $[\text{Pd}_2(\text{mipk})_2(\mu\text{-1-Methy})_2]^{2+}$ (mipk = 1-methyl-

imidazol-2-yl pyridin-2-yl ketone).²¹ In the related complex $[\text{Pd}_2(\text{bpm})_2(\mu\text{-1-Methy})_2]^{2+}$ (bpm = bis(pyridine-2-yl)-methane), the 1-methylthyminato bridged ligands are arranged in a head-to-head fashion.²² In complex **1** both Pd atoms are slightly out of their coordination planes. The bite range of the 1-methylthyminato bases [$\text{N}(2)\cdots\text{O}(2) = 2.290 \text{ Å}$; $\text{N}(5)\cdots\text{O}(3) = 2.277 \text{ Å}$] is considerably smaller than the metal–metal distance, resulting in a dihedral angle between the two square-planar metal coordinating planes of $37.92(8)^\circ$, giving a basket-shaped eight-membered ring. The cyclometalated rings are puckered with the nitrogen atom significantly out of the plane defined by the palladium and carbon atoms, a feature which is quite commonly observed in cyclometalated dmba complexes. The Pd–N(sp^2) distances (2.056 and 2.068 Å) are similar to values found for 1-Methy-bridged compounds such as $[\text{Pd}_2(\text{mipk})_2(\mu\text{-1-Methy})_2]^{2+}$ (2.043 and 2.045 Å).²¹ However the Pd–O (2.150 and 2.133 Å) distances in complex **1** are higher than the corresponding lengths (2.010 and 2.012 Å) in the above-mentioned complex.²¹ A number of cyclometalated dmba complexes with nitrogen and oxygen ligands have been structurally characterized. In all instances the nitrogen atoms occupy trans sites at the metal with oxygen trans to carbon, as indeed is observed for **1**. The Pd–N(sp^3) distances in **1**, $2.095(2)$ and $2.074(3) \text{ Å}$, are comparable with those in $[\{\text{Pd}(\text{dmba})\}_2(\mu\text{-MHC}(\text{Ph})\text{O})_2]$ ($2.079(3)$ and $2.087(3) \text{ Å}$).¹⁴ The Pd–C distances in **1** ($1.970(3)$ and $1.967(3) \text{ Å}$) also lie within the range normal for palladium dmba complexes. Dinuclear neutral molecules of complex **1** are stacked to give centrosymmetric pairs, as shown in Figure 2, due to intermolecular $\pi\text{-}\pi$ interactions between 1-Methy ligands ($\text{C}13\cdots\text{C}13$: 3.418 Å). The planes of the ligands are parallel, the distance between both planes being $3.403(4) \text{ Å}$ and the distance between centroids being 4.614 Å . The angle between the ring normal and the centroid vector is 43° .

The crystal structure of the dimeric complex **3**· 2CHCl_3 is shown in Figure 3. Selected interatomic distances and angles are listed in Table 2. To our knowledge, this compound represents the first example of a (1-methylcytosinato)-palladium(II) cyclometalated complex being fully characterized by X-ray diffraction. Each Pd atom is in a distorted square-planar arrangement. The metals are bridges by two cytosinate anions through the endocyclic N(3) and the deprotonated amino group, N(4), in a head-to-tail arrangement and anti structure. The $\text{N}(2)\cdots\text{N}(3)$ and $\text{N}(5)\cdots\text{N}(7)$ bite distances (2.329 and 2.322 Å , respectively) are considerably shorter than the intramolecular Pd···Pd distance of $3.0056(6) \text{ Å}$, which is close to that found in $[\text{Pd}_2(\text{NH}_3)_4(\mu\text{-1-Mecyt})_2]^{2+}$ ($2.948(1) \text{ Å}$).²³ As a consequence, the coordination planes of the two metal atoms form a dihedral angle of $31.6(2)^\circ$. The dihedral angle between the two pyrimidine planes is $86.1(2)^\circ$. The bond lengths and angles within the cytosinate rings do not differ significantly from published

(21) Engelking, H.; Krebs, B. *J. Chem. Soc., Dalton Trans.* **1996**, 2409.

(22) Mock, C.; Puscasu, I.; Rauterkus, M. J.; Tallen, G.; Wolff, J. E. A.; Krebs, B. *Inorg. Chim. Acta* **2001**, *319*, 109.

(23) Navarro-Ranninger, C.; Montero, E. I.; López-Solera, I.; Masaguer, J. R.; Lippert, B. *J. Organomet. Chem.* **1998**, *558*, 103.

(20) CCDC CSD version 5.27, Nov 2005, update Jan 2006.

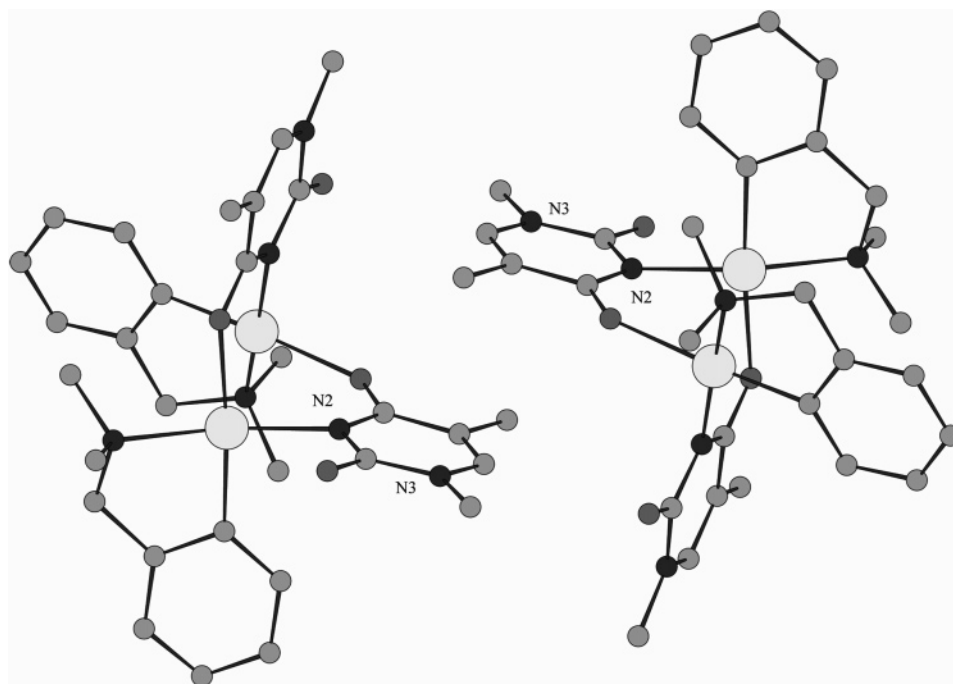


Figure 2. Centrosymmetric dimer-of-dimers arrangement of **1**.

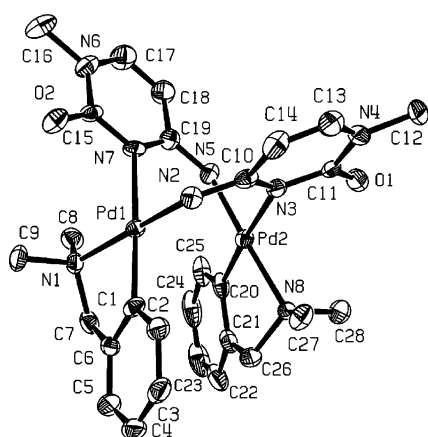


Figure 3. ORTEP of complex **3**·2CHCl₃, showing the atom-numbering scheme. Displacement ellipsoids are drawn at the 50% probability level.

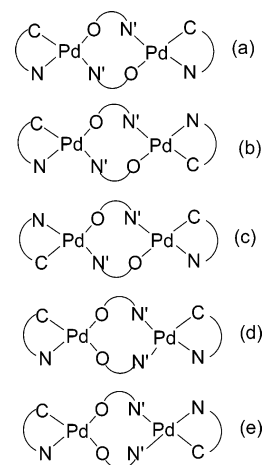
Table 2. Selected Distances (Å) and Bond Angles (deg) for Complex **3**·2CHCl₃

Bond Distances		Bond Angles	
Pd(1)–C(1)	1.978(5)	C(1)–Pd(1)–N(2)	93.0(2)
Pd(1)–N(2)	2.015(4)	C(1)–Pd(1)–N(1)	81.8(2)
Pd(1)–N(1)	2.097(4)	N(2)–Pd(1)–N(1)	172.45(18)
Pd(1)–N(7)	2.153(4)	C(1)–Pd(1)–N(7)	175.30(19)
Pd(2)–C(20)	1.984(5)	N(2)–Pd(1)–N(7)	91.39(17)
Pd(2)–N(8)	2.096(4)	N(1)–Pd(1)–N(7)	93.92(16)
Pd(2)–N(3)	2.167(4)	C(20)–Pd(2)–N(5)	93.5(2)
Pd(2)–N(5)	2.018(4)	C(20)–Pd(2)–N(8)	81.7(2)
Pd(1)···Pd(2)	3.0056(6)	N(5)–Pd(2)–N(8)	172.59(18)
		C(20)–Pd(2)–N(3)	175.83(19)
		N(5)–Pd(2)–N(3)	90.45(17)
		N(8)–Pd(2)–N(3)	94.25(16)

values.²⁴ Furthermore, hydrogen bonding is clearly a major factor in holding the crystal together (distance C30–H30···O2, 3.063 Å; distance C29–H29···O1, 3.261 Å; distance N5–H5A···C4, 3.237 Å).

NMR Data for Complexes 1–3. The ¹H NMR spectra of these compounds (see Experimental Section) show that

Scheme 3



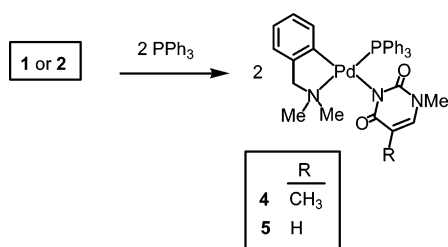
both the *N*-methyl and the CH₂ groups of the dmbs are diastereotopic, two separate signals being observed for the former and an AB quartet for the latter. Therefore, there is no plane of symmetry in the Pd coordination plane.²⁵ A folded “basket” structure related to that observed in acetato-bridged dimers is likely.^{14,26} Since both C₆H₄CH₂NMe₂ and the nucleobases anions are unsymmetrical, there are five possible diastereomers for the dimeric complexes, two of them with head-to-head (d and e, Scheme 3, for complexes **1** and **2**) and the other three with head-to-tail arrangements (a–c) of the bridging nucleobase anionic ligands, but only one isomer is present in solution at room temperature, perhaps due to the fact that the ligand dmbs exerts very

(24) Faggiani, R.; Lippert, B.; Lock, C. J. L.; Speranzini, R. A. *J. Am. Chem. Soc.* **1981**, *103*, 1111.

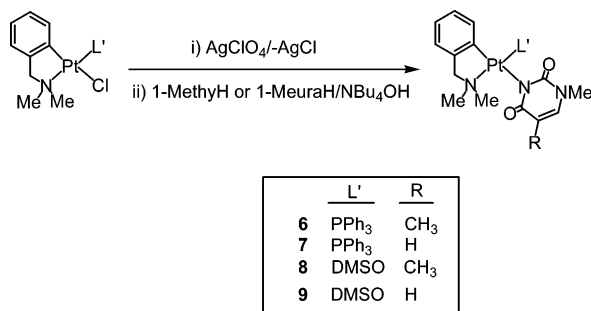
(25) Deeming, A. J.; Mean, M. N.; Bates, P. J.; Hursthouse, M. B. *J. Chem. Soc., Dalton Trans.* **1978**, 1490.

(26) Deeming, A. J.; Mean, M. N.; Bates, P. J.; Hursthouse, M. B. *J. Chem. Soc., Dalton Trans.* **1988**, 2193.

Scheme 4



Scheme 5



different trans influences through its C and N atoms.²⁶ The observation of a unique resonance for the MeN(1) and MeC(5) protons of the 1-methylthyminato ligands in the ¹H NMR spectrum of complex **1** (at δ 3.32 and 1.77, respectively), together with the observed C₆H₄CH₂NMe₂ resonances, are consistent with only the head-to-tail structures (b or c, Scheme 3) (the assignments were unambiguously confirmed by ¹H–¹³C COSY experiments for complexes **1–3**). In complex **2** a unique resonance pattern for the H(6), H(5), and MeN(1) protons of the 1-methyluracilato ligands is observed. Furthermore, we should expect that the O atom would be trans to the carbon atom of the C₆H₄CH₂NMe₂ chelate (an anti arrangement c) by analogy to the imidate complexes [(C,N)Pd(μ -NCOC₂H₄CO)]₂ (C,N = *o*-C₆H₄CH₂NMe₂, *o*-C₆H₄CH=NPh)²⁷ and the amidate complex [(C,N)-Pd(μ -NHC(Ph)O)]₂ (C,N = *o*-C₆H₄CH₂NMe₂).¹⁴ All this suggests that c is the most probable structure for the binuclear complexes **1** and **2** in solution, which is in accordance with the crystal structure of complex **1**.

The ¹H NMR spectrum of complex **3** shows the exocyclic amine proton of 1-Mecyt as a singlet at δ 5.13. The comparison of the chemical shifts observed for the aromatic 1-Mecyt protons in **3** (5.50 and 6.55 ppm for H(5) and H(6) and free 1-MecytH (5.60 and 7.55 ppm for H(5) and H(6), respectively) are also consistent with 1-Mecyt acting as a bridged ligand through N(3) and N(4) atoms.^{23,28} This point is also consistent with the X-ray determination of the crystal structure of complex **3** described above.

Monomeric Metal Complexes [M(dmba)(L)(L')] (M = Pd or Pt; L = 1-Methyl or 1-Meura; L' = PPh₃ or DMSO). The reactions of **1** and **2** with PPh₃ (in a 1:2 molar ratio) in dichloromethane at room temperature yield the monomeric complexes [Pd(dmba)(L)(PPh₃)] [L = 1-Methyl (**4**) and L = 1-Meura (**5**)], respectively (Scheme 4).

The platinum analogous complexes have been prepared from the corresponding chloro precursor [PtCl(dmba)(L')] (L' = PPh₃ or DMSO) (Scheme 5). After precipitation of

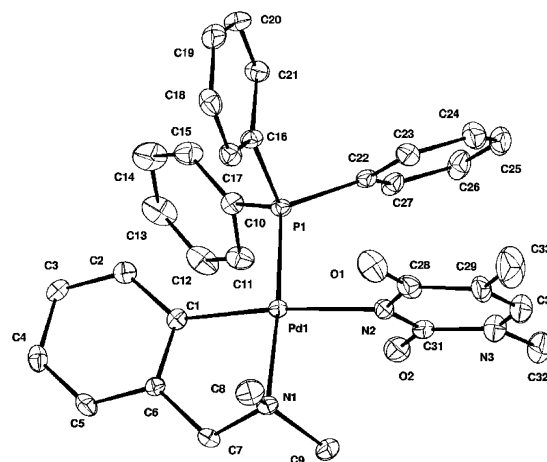


Figure 4. ORTEP of complex **4**·3CHCl₃, showing the atom-numbering scheme. Displacement ellipsoids are drawn at the 50% probability level.

Table 3. Selected Distances (Å) and Bond Angles (deg) for Complex **4**·3CHCl₃

Bond Distances		Bond Angles	
Pd(1)–C(1)	2.007(7)	C(1)–Pd(1)–N(2)	173.8(3)
Pd(1)–N(2)	2.107(6)	C(1)–Pd(1)–N(1)	82.1(3)
Pd(1)–N(1)	2.149(6)	N(2)–Pd(1)–N(1)	92.0(2)
Pd(1)–P(1)	2.2385(18)	C(1)–Pd(1)–P(1)	94.0(2)
		N(2)–Pd(1)–P(1)	91.95(17)
		N(1)–Pd(1)–P(1)	175.95(17)

AgCl by addition of AgClO₄ in a 1:1 molar ratio in acetone, the solvento complexes [Pt(dmba)(L')(Me₂CO)]ClO₄ generated in situ react with 1 equiv of 1-MethylH or 1-MeuraH and [NBu₄]OH to give the neutral complexes [M(dmba)(L')(L)] (L = 1-Methyl or 1-Meura; **6–9**).

Complexes **4–9** are white, air-stable solids that decompose on heating above 237 °C. Evidence for the coordination of the metal to the deprotonated imidic N3 atom comes from the lowered C=O stretching frequencies (1705 and 1685 cm⁻¹ in N1-methylthymine), which reflects the longer carbonyl bonds due to deprotonation of the N3–H group.¹⁰

Crystal Structures of 4·3CHCl₃ and 6. The structure of **4**·3CHCl₃ is shown in Figure 4. Selected bond distances and bond angles are given in Table 3. Coordination at palladium is approximately square planar, although the angles around palladium deviate from 90° due to the bite of the cyclo-metalated ligand. The C(1)–Pd–N(1) angle of 82.1(3)° is within the normal range for such complexes.^{14,29} The PPh₃ ligand is trans to the nitrogen donor due to the difficulty of coordinating a phosphine trans to an aryl ligand in palladium complexes (i.e. the destabilizing effect known as *transphobia*).³⁰ The Pd atom coordinates N3 of thyminato. The Pd–N3 distance is 2.107 Å, suggesting a strong interaction between the metal and the imidic nitrogen.¹⁰ The Pd–C bond length is essentially the same as that reported in [Pd(*o*-C₆H₄CH₂NMe₂)(PCy₃)(TFA)].²⁹ The complex **4**·3CHCl₃ has

(27) Adams, H.; Bailey, N.; Briggs, T. N.; McCleverty, J. A.; Colquhoun, H. M.; Williams, D. J. *J. Chem. Soc., Dalton Trans.* **1986**, 813.

(28) Krumm, M.; Mutikainen, I.; Lippert, B. *Inorg. Chem.* **1991**, *30*, 884.

(29) Bedford, R. B.; Cazin, C. S. J.; Coles, S. J.; Gelbrich, T.; Horton, P. N.; Hursthouse, M. B.; Light, M. E. *Organometallics* **2003**, *22*, 987.

(30) Vicente, J.; Arcas, A.; Bautista, D.; Jones, P. G. *Organometallics* **1997**, *16*, 2127.

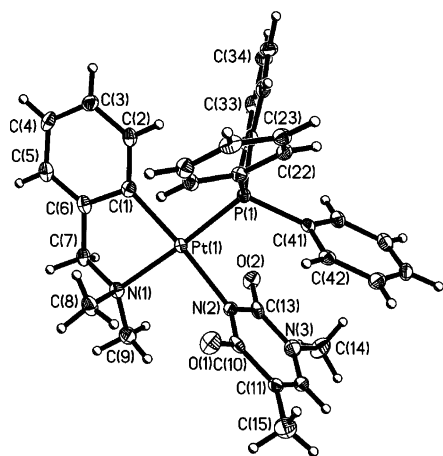


Figure 5. ORTEP of complex **6**, showing the atom-numbering scheme. Displacement ellipsoids are drawn at the 50% probability level.

Table 4. Selected Distances (Å) and Bond Angles (deg) for Complex **6**

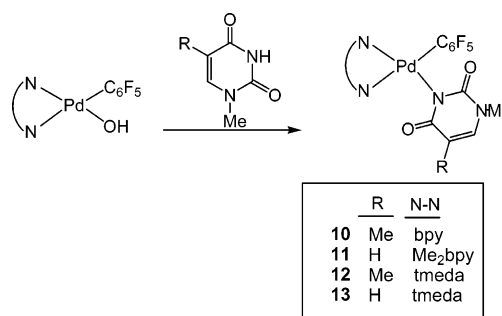
Bond Distances		Bond Angles	
Pt(1)–C(1)	2.014(4)	C(1)–Pt(1)–N(2)	172.59(12)
Pt(1)–N(2)	2.122(3)	C(1)–Pt(1)–N(1)	81.79(13)
Pt(1)–N(1)	2.130(3)	N(2)–Pt(1)–N(1)	92.62(11)
Pt(1)–P(1)	2.2091(9)	C(1)–Pt(1)–P(1)	95.47(11)
		N(2)–Pt(1)–P(1)	90.56(8)
		N(1)–Pt(1)–P(1)	173.71(8)

two molecules of chloroform hydrogen bonded to the thymine ligand (distance C34–H34···O1, 3.016 Å; distance C36–H36···O2, 2.725 Å). Remarkably, there is also an intermolecular C–Cl···O–C interaction³¹ (distance O1···Cl6, 3.153 Å; angle O1···Cl6–C35, 161.8°; angle C28–O1···Cl6, 114.6°). Furthermore, there is an intramolecular interaction by phenyl–thyminato π -stacking (N2···C22, 3.115 Å; C23···C28, 3.217 Å). The planes of both rings make an angle of 21.4°, with an interplanar distance (average of the two distances between the mean plane of one ring and the centroid of the other) of 3.375 Å, a center-to-center distance of 3.649 Å, and a deviation of the center–center line of the perpendicular of the plane of 18.1(4)° (thymine ring) and 35.1(4)° (phenyl ring).

The structure of **6** is shown in Figure 5. Selected bond distances and bond angles are given in Table 4. The platinum atom displays approximately square planar coordination. The X-ray crystallographic data revealed that Pt coordinates N3 of thymine. The plane of the Methyl ligand is approximately perpendicular to the platinum coordination plane. The PPh₃ ligand is trans to the nitrogen donor. There is an intramolecular interaction by phenyl–thyminato π -stacking (N2···C41, 3.063 Å; C10···C42, 3.270 Å; C13···C46, 3.331 Å). The planes of both rings make an angle of 20.9°, with an interplanar distance (average of the two distances between the mean plane of one ring and the centroid of the other) of 3.4189 Å, a center-to-center distance of 3.566 Å, and a deviation of the center–center line of the perpendicular of the plane of 11.6° (thymine ring) and 20.2° (phenyl ring). There is also a C–H···O bond link (distance C45–H45···O1[#], 3.180(5) Å; angle, 143.5°).

(31) Lommerse, J. P. M.; Stone, A. J.; Taylor, R.; Allen, F. H. *J. Am. Chem. Soc.* **1996**, *118*, 3108.

Scheme 6



NMR Data for Complexes 4–9. The ¹H NMR spectra of complexes **4–9** show that both the *N*-methyl and the CH₂ groups of the dmbs are diastereotopic, two separate signals being observed for the former and an AB quartet for the latter. Therefore, there is no plane of symmetry in the metal coordination plane. In complexes **4–7** the PPh₃-trans-to-NMe₂ ligand arrangement in the starting products^{32,33} is preserved, after chlorine abstraction and 1-Methyl or 1-Meura coordination, as can be inferred from the small, but significant, coupling constants ⁴J_{P–H} (ranging from 1.5 to 3.0 Hz) of the NMe₂ and the CH₂N protons with the phosphorus atom.^{34,35} Two different signals are also observed for the DMSO ligand in the ¹³C{¹H} NMR spectra of complexes **8** and **9**. A unique resonance is observed in the ¹⁹⁵Pt NMR spectra of complexes **6–9**. A comparison of ¹H and ¹³C NMR data for complex **4** and the related complex *trans*-[PdCl(1-Methyl)(PPh₃)₂]¹⁰ suggested that the coordination of the metal occurred on the N3 atom of the nucleobase as observed in the solid state.

Complexes [Pd(C₆F₅)(N–N)(L)] (L = 1-Methyl or 1-Meura). In acetone, the hydroxo complexes [Pd(N–N)(C₆F₅)(OH)] [N–N = bpy (2,2'-bipyridyl), Me₂bpy (4,4'-dimethyl-2,2'-bipyridyl), or tmeda (*N,N,N',N'*-tetramethylethylenediamine)] react with 1 equiv of 1-MethylH or 1-MeuraH to yield the corresponding complexes [Pd(N–N)(C₆F₅)(L)] (**10–13**) (Scheme 6) in 65–73% yields. The structures were assigned on the basis of microanalytical, IR, and ¹H and ¹⁹F NMR data and mass spectra (positive-ion FAB). The IR spectra show the characteristic absorptions of the C₆F₅ group³⁶ at 1630, 1490, 1450, 1050, and 950 cm^{–1} and a single band at ca. 800 cm^{–1} derived from the so-called X-sensitive mode³⁷ in C₆F₅X (X = halogen) molecules, which is characteristic of the presence of only one C₆F₅ group in the coordination sphere of the palladium atom and behaves like a ν (M–C) band.³⁸

(32) Deeming, A. J.; Rothwell, I. P.; Hursthouse, M. B.; New, L. *J. Chem. Soc., Dalton Trans.* **1978**, 1490.

(33) Meijer, M. D.; Kleij, A. W.; Williams, B. S.; Ellis, D.; Lutz, M.; Spek, A. L.; van Klink, G. P. M.; van Koten, G. *Organometallics* **2002**, *21*, 264.

(34) Braunstein, P.; Matt, D.; Dusausoy, Y.; Fischer, J.; Mitschler, A.; Ricard, L. *J. Am. Chem. Soc.* **1981**, *103*, 5115.

(35) Falvello, L. R.; Fernández, S.; Navarro, R.; Urriolabeitia, E. P. *Inorg. Chem.* **1997**, *36*, 1136.

(36) Long, D. A.; Steele, D. *Spectrochim. Acta* **1963**, *19*, 1955.

(37) Maslowski, E. *Vibrational Spectra of Organometallic Compounds*; Wiley: New York, 1977; p 437.

(38) Alonso, E.; Forniés, J.; Fortuño, C.; Tomás, M. *J. Chem. Soc., Dalton Trans.* **1995**, 3777.

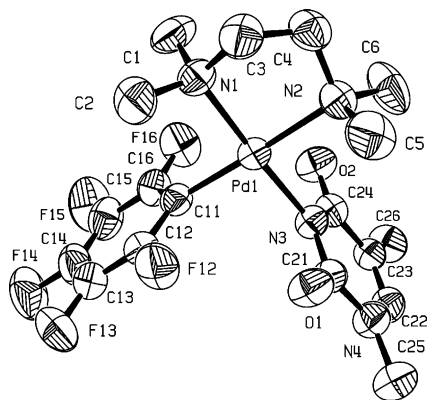


Figure 6. ORTEP of complex **12**, showing the atom-numbering scheme. Displacement ellipsoids are drawn at the 50% probability level.

Table 5. Selected Distances (Å) and Bond Angles (deg) for Complex **12**

Bond Distances		Bond Angles	
Pd(1)–C(11)	2.012(5)	C(11)–Pd(1)–N(3)	90.11(17)
Pd(1)–N(3)	2.038(4)	C(11)–Pd(1)–N(1)	93.12(17)
Pd(1)–N(1)	2.089(4)	N(3)–Pd(1)–N(1)	176.71(15)
Pd(1)–N(2)	2.123(4)	C(11)–Pd(1)–N(2)	177.74(16)
		N(3)–Pd(1)–N(2)	92.14(16)
		N(1)–Pd(1)–N(2)	84.63(17)

Crystal Structure of 12. A drawing of complex **12** is shown in Figure 6 with selected bond lengths and angles listed in Table 5. The Methy ligand is approximately perpendicular to the coordination plane, with angles between planes of $89.5(1)^\circ$. The Pd–N thymine distance (Pd(1)–N(3): 2.038(4) Å) is shorter than that observed in complex **4**·3CHCl₃, suggesting a very strong interaction between the metal and the imidic nitrogen.¹⁰ The different Pd–N tmeda distances (Pd(1)–N(1), 2.089(4) Å; Pd(1)–N(2), 2.123(4) Å) are in agreement with the higher trans influence of the group C₆F₅ compared to the thymine. The Pd–C₆F₅ bond length (2.012(5) Å) is in the range found in the literature for pentafluorophenyl–palladium complexes.³⁹ The chelate angle N(1)–Pd(1)–N(2) is $84.63(17)^\circ$. There are also intermolecular π – π interactions between Methy ligands, so molecules of complex **12** are stacked to give centrosymmetric pairs, as shown in Figure 7. It is a slipped packing with a deviation of the center–center line of the perpendicular of the plane of 24.7° ; the interplanar distance is 3.384 Å.

NMR Data for Complexes 10–13. The characteristic resonances of the chelate ligands are observed in the ¹H NMR spectra,^{15,17,39–41} and the assignments presented in the Experimental Section are based on the atom numbering given in Scheme 7. The ¹⁹F NMR spectra of complexes **10–13** at room temperature show hindered rotation of the C₆F₅ ring around the Pd–C bond, and two separate signals are observed for the *o*-fluorine atoms but only one for the *p*-fluorine atom.

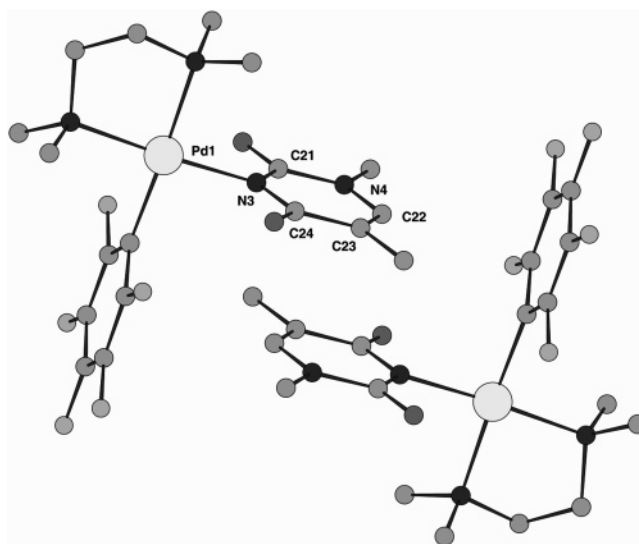
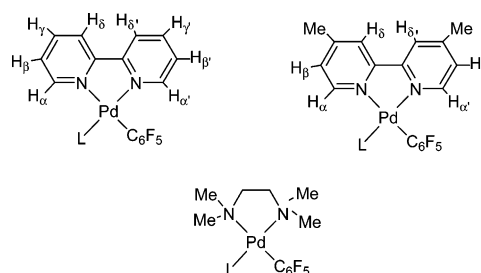
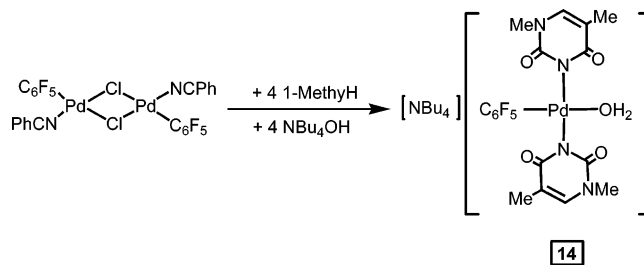


Figure 7. π – π interactions in complex **12**.

Scheme 7



Scheme 8



Complex [NBu₄][Pd(C₆F₅)(H₂O)(1-Methy)₂]. The palladium bis(thymine) complex [NBu₄][Pd(C₆F₅)(H₂O)(1-Methy)₂] (**14**) has been prepared by reaction in acetone of the halo-complex [$\text{Pd}(\text{C}_6\text{F}_5)(\text{NCPH})(\mu\text{-Cl})_2$] with [NBu₄]OH and 1-Methylamine in the molar ratio 1:4:4, as shown in Scheme 8.

The new complex has been characterized by elemental analysis and spectroscopic data.

Crystal Structure of 14·H₂O. The structure of compound **14**·H₂O is shown in Figure 8, and selected bond lengths and angles are in Table 6. To the best of our knowledge this is the first crystal structure of a monomeric palladium bis(thymine) complex.²⁰ A trans geometry around the Pd center is observed. For example, the angle N(1)–Pd(1)–N(3) is $177.37(14)^\circ$. The crystal structure of the related bis(imidato) complex *trans*-[[Pd(C₆F₅)(H₂O)(succinimidate)₂] \cdot H₂O has been recently reported.¹⁹ The Pd–OH₂ distances are similar to those found in [Pd(C₆F₅)(AsPh₃)(H₂O)₂][CF₃SO₃]⁴² and [NBu₄][Pd(C₆F₅)(H₂O)(succinimidate)₂] \cdot

(39) Forniés, J.; Martínez, F.; Navarro, R.; Urriolabeitia, E. P. *J. Organomet. Chem.* **1995**, 495, 185.

(40) Byers, P. K.; Canty, A. J. *Organometallics* **1990**, 9, 210.

(41) Ruiz, J.; Cutillas, N.; Vicente, C.; Villa, M. D.; López, G.; Lorenzo, J.; Avilés, F. X.; Moreno, V.; Bautista, D. *Inorg. Chem.* **2005**, 44, 7365.

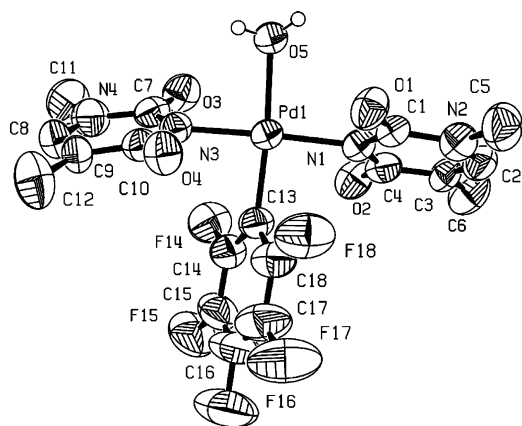


Figure 8. ORTEP of complex **14**·H₂O, showing the atom-numbering scheme. Displacement ellipsoids are drawn at the 50% probability level.

Table 6. Selected Distances (Å) and Bond Angles (deg) for Complex **14**·H₂O

Bond Distances		Bond Angles	
Pd(1)–C(13)	1.981(5)	C(13)–Pd(1)–N(3)	87.28(18)
Pd(1)–N(3)	2.034(4)	C(13)–Pd(1)–N(1)	90.14(18)
Pd(1)–N(1)	2.056(4)	N(3)–Pd(1)–N(1)	177.37(14)
Pd(1)–O(5)	2.140(3)	C(13)–Pd(1)–O(5)	174.62(17)
		N(3)–Pd(1)–O(5)	88.17(15)
		N(1)–Pd(1)–O(5)	94.43(15)

H₂O.¹⁹ An interesting feature of the crystal structure is the presence of dimeric units of [Pd(C₆F₅)(H₂O)(1-Methy)₂]₂·2H₂O (Figure 9) due to OH···O hydrogen bonds (Table 7) involving the thymine ligands, the coordinated water molecules, and the water molecules of crystallization. There are also short intermolecular contacts (O1···N3 3.062 Å).

NMR Data for Complex 14. The ¹H NMR spectrum of complex **14** exhibits a unique set of resonances for the thymine ligands which suggests a trans isomer in acetone-*d*₆ solution. No isomerization process was observed when a solution of **14** was kept in solution in acetone-*d*₆ for a prolonged period. The trans structure of **14** is in accordance with the single-crystal X-ray diffraction data given above. As expected, three signals with relative intensities of 2:1:2 (2F_{ortho}:1F_{para}:2F_{meta}) are found in the ¹⁹F NMR spectrum of **14**.

Biological Assays. Circular Dichroism Spectroscopy. The circular dichroism (CD) spectra of calf thymus DNA alone and incubated with the ligands 1-MethyH and 1-MeuraH and its platinum(II) compounds at 37 °C for 24 h with several molar ratios were recorded.

The free ligands 1-MethyH and 1-MeuraH did not significantly modify either the ellipticity of the bands or their position. In contrast, the changes in ellipticity and wavelength caused by the new platinum complexes are significant (Table 8). Complexes **6** and **7** reduce the ellipticity of the positive band with increasing values of *r*_i. This phenomenon is indicative of B → C transformation with increasing winding of the DNA helix by rotation of the bases.^{43–46} Complexes

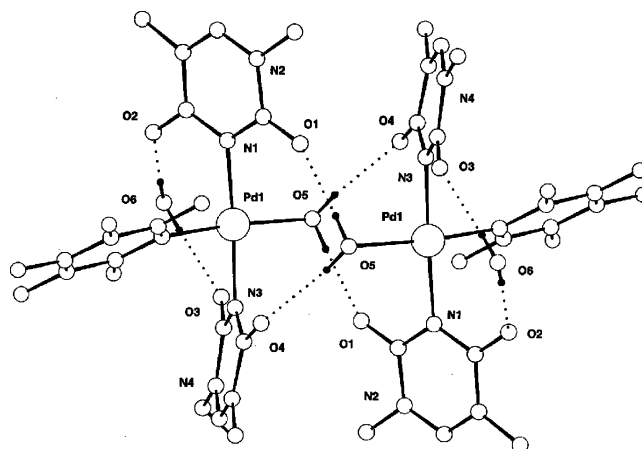


Figure 9. Dimeric structure of [Pd(C₆F₅)(H₂O)(1-Methy)₂]₂·2H₂O, showing the hydrogen bonds.

Table 7. Hydrogen Bonds for **14**·H₂O (Å and deg)

D–H···A	<i>d</i> (D–H)	<i>d</i> (H···A)	<i>d</i> (D···A)	–(DHA)
O(6)–H(62)···O(3)	0.79(2)	1.99(2)	2.777(6)	178(6)
O(6)–H(61)···O(2)	0.79(2)	2.00(2)	2.790(6)	177(5)
O(5)–H(51)···O(1) ^{#1}	0.81(2)	1.94(2)	2.746(5)	175(6)
O(5)–H(52)···O(4) ^{#1}	0.79(2)	2.02(2)	2.799(5)	167(5)

^a Symmetry transformations used to generate equivalent atoms: (#1) –*x* + 1, –*y* + 1, –*z* + 1.

Table 8. CD Spectral Data for DNA for Different *r*_i Values (Molar Ratios)

compd	<i>r</i> _i	λ _{max} (nm)	10 ^{–3} θ _{max} (deg·cm ² ·dmol ^{–1})	λ _{min} (nm)	10 ^{–3} θ _{min} (deg·cm ² ·dmol ^{–1})
DNA		275.2	1.89	246.2	–2.21
6	0.1	273.0	1.94	246.0	–1.94
	0.3	275.0	1.89	247.0	–2.03
	0.5	273.8	1.83	246.0	–1.97
7	0.1	276.4	1.74	245.8	–2.01
	0.3	277.2	1.62	247.0	–1.62
	0.5	275.6	1.50	247.4	–1.72
8	0.1	247.2	2.06	246.6	–1.94
	0.3	277.6	2.14	248.6	–2.04
	0.5	279.6	2.16	247.8	–2.02
9	0.1	275.0	2.03	246.2	–1.97
	0.3	275.4	2.08	246.0	–2.03
	0.5	276.6	2.18	247.8	–1.96

8 and **9** induce modifications in the secondary structure of DNA in a way different. In this case, the two complexes increase the ellipticity of the positive band with increasing values of *r*_i. These changes were similar to those produced by cisplatin.⁴⁷ These modifications are probably due to opening of the helix upon the formation of DNA intrastrand adducts.⁴⁸

Gel Electrophoresis of Compound–pBR322 Complexes. The influence of the compounds on the tertiary structure of DNA was determined by their ability to modify the electrophoretic mobility of the covalently closed circular (ccc) and open (oc) forms of pBR322 plasmid DNA. The

(42) Ruiz, J.; Florenciano, F.; Vicente, C.; Ramírez de Arellano, M. C.; López, G. *Inorg. Chem. Commun.* **2000**, 3, 73.

(43) Macquet, J. P.; Butour, J. L. *Biochimie* **1978**, 60, 901.

(44) Brabec, V.; Kleinwächter, V.; Butour, J.; Johnson, M. P. *Biophys. Chem.* **1990**, 35, 129.

(45) Cervantes, G.; Prieto, M. J.; Moreno, V. *Met. Based Drugs* **1997**, 4, 9.

(46) Cervantes, G.; Marchal, S.; Prieto, M. J.; Pérez, J. M.; González, V. M.; Alonso, C.; Moreno, V. *J. Inorg. Biochem.* **1999**, 77, 197.

(47) Riera, X.; Moreno, V.; Freisinger, E.; Lippert, B. *Inorg. Chim. Acta* **2002**, 253–264.

(48) Moradell, S.; Lorenzo, J.; Rovira, A.; Robillard, M. S.; Avilés, S.; Moreno, V. *J. Inorg. Biochem.* **2003**, 96, 500.

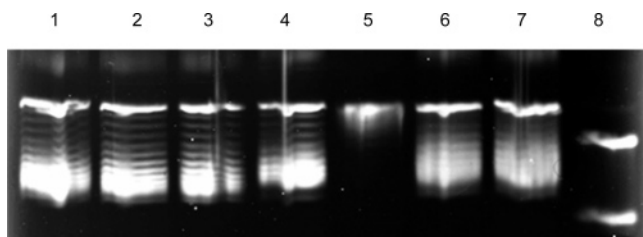


Figure 10. Modification of the gel electrophoretic mobility of pBR322 plasmid incubated with 1-MethyH and 1-MeuraH and their platinum compounds: lane 1, pBR; lane 2, MethyH; lane 3, MeuraH; lane 4, complex **6**; lane 5, complex **7**; lane 6, complex **8**; lane 7, complex **9**; lane 8, complex pBR-cisplatin.

platinum complexes and the free ligands 1-MethyH and 1-MeuraH were incubated at the molar ratio $r_1 = 0.50$ with pBR322 plasmid DNA at 37 °C for 24 h. Representative gel obtained for the Pt complexes **6–9** are shown in Figure 10. The behavior of the gel electrophoretic mobility of both forms, ccc and oc, of pBR322 plasmid and the DNA-cisplatin adduct is consistent with previous reports.⁴⁹ No changes were observed in sample incubated with the free ligands 1-MethyH and 1-MeuraH. When the pBR322 was incubated with the platinum compounds **6** (lane 4), **7** (lane 5), **8** (lane 6), and **9** (lane 7) a retard in the mobility of ccc form was observed.

AFM Study of Compound-pBR322 Complexes. Consequently to the behavior observed in the electrophoretic

Table 9. IC₅₀ (μ M) for Cisplatin and Complexes **6–9** for the Tumor Cell Line HL-60

complex	24 h	72 h
cisplatin	15.61	2.15
6	0.692	0.729
7	0.674	0.643
8	1.614	0.935
9	1.537	0.782

mobility, the complexes **6–9** modify the morphology of the pBR322 DNA and the ccc forms are predominant in the pictures (Figure 11). In all cases the complexes seem to modify the morphology of the pBR322 DNA in mode similar to that of cisplatin.^{41,45,50–52} The platinum complexes attached to DNA cause kinks and cross-linking in the plasmid forms. The background of the Figure 11d indicates the presence of a layer of water molecules from the environment over the mica surface which can be the origin of the aggregation of the forms.

Cytotoxicity Studies. The in vitro growth inhibitory effect of the platinum complexes **6–9** and cisplatin was evaluated in HL-60 human tumor cell line. As listed in Table 9, both at 24 and 72 h incubation times all of the new platinum complexes were more active than cisplatin. In fact, at a short incubation time (24 h) complexes **6** and **7** were about 20-fold more active than cisplatin toward HL60 cells. After 72 h of incubation time, complexes **6–9** were also about 3-fold more active than cisplatin.

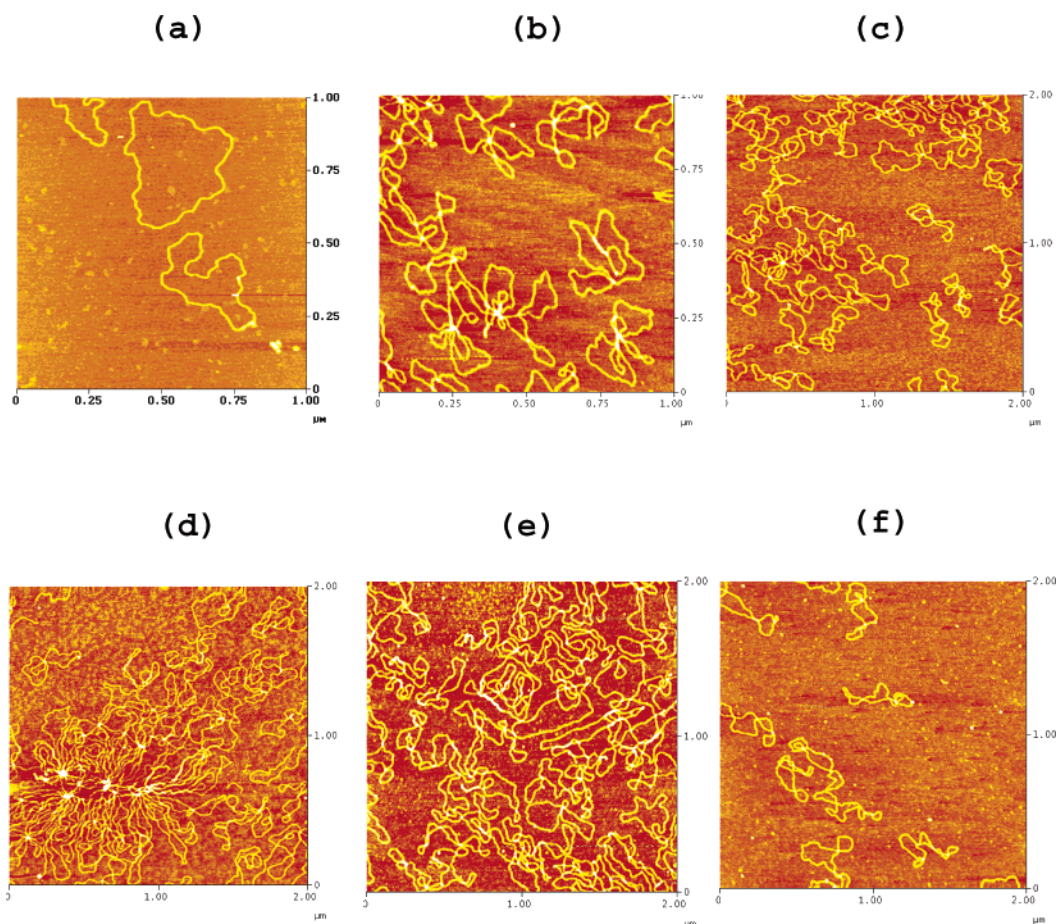


Figure 11. TMAFM image corresponding to (a) pBR322, (b) pBR-cisplatin, (c) pBR-complex **6**, (d) pBR-complex **7**, (e) pBR-complex **8**, and (f) pBR-complex **9**.

Table 10. Percentages of Vital Cells, Apoptotic Cells, Dead Cells, and Damaged Cells after Treatment of a HL-60 Cell Population with Cisplatin and Complexes 6–9 for 24 h

treatment (IC ₅₀ 24 h, mM)	% vital cells (R1)	% apoptotic cells (R2)	% dead cells (R3)	% damaged cells (R4)
control	85.39	8.43	5.95	0.24
cisplatin (15.6)	53.89	40.68	4.89	0.55
6 (0.692)	63.38	27.77	8.48	0.38
7 (0.674)	68.55	19.61	10.26	1.58
8 (1.614)	46.38	32.52	16.05	5.05
9 (1.537)	54.29	21.25	12.97	1.50

In Vitro Apoptosis Assay. The most common and well-defined form of programmed cell death is apoptosis, which is a physiological cell suicide program that is essential for the maintenance of tissue homeostasis in multicellular organism. In contrast to the self-contained nature of apoptotic cell death, necrosis is a messy, unregulated process of traumatic cell destruction, which is followed by the release of intracellular components. During the past decade, cell biology as well as oncology research has focused on this latter process of programmed cell death, or apoptosis. It is anticipated that understanding of the basic mechanisms that underlie apoptosis will offer potential new targets for therapeutic treatment of diseases.⁵³

The type of cell death induced by the new complexes was investigated by Annexin V/PI apoptosis assay in a flow cytometer. The results obtained for the different complexes at 24 h of incubation time were compared with those for cisplatin. With all drugs, apoptosis was observed and the percentages are presented in Table 10. Exposure of cells to cisplatin and complexes **6** and **8** resulted in a significant induction of apoptosis (30–40% of apoptotic cells) compared with that induced by complexes **7** and **9** (20%). However, an additional population of cells appeared to be dying by necrosis or late apoptosis when HL60 cells were exposed to complexes **6–9**.

Reactions of the Platinum Complexes 6 and 8 with 9-Ethylguanine and Guanosine. To gain insight into the reactivity of the new platinum complexes, the reactions of complex **8** with an excess of 9-ethylguanine and guanosine were followed by ¹H NMR at physiological temperature and pH (see Experimental Section). In both cases the reactions are very fast and in less than 5 min the formation of the corresponding complexes [Pt(dmba)(DMSO)(L)]⁺ (L = 9-EtG or guanosine) is completed. No further changes were observed after 2 h. In both cases the signal for the H(8) of the free guanine or guanosine moves downfield upon coordination. In the reaction of complex **8** with the model nucleobase 9-ethylguanine two different signals were observed both for the coordinated DMSO and the NMe₂ of the dmba (Experimental Section and Supporting Information).

The reaction of complex **6** with an excess of 9-ethylguanine is also fast and yields the formation of [Pt(dmba)(PPh₃)(9-EtG)]⁺.

Conclusions

New Pd(II) and Pt(II) organometallic complexes with the anions of the model nucleobases 1-methylthymine, 1-methyluracil, and 1-methylcytosine have been prepared. The crystal structures of [Pd(dmba)(μ-1-Methy)]₂, [Pd(dmba)(μ-1-Mecyt)]₂·2CHCl₃, [Pd(dmba)(1-Methy)(PPh₃)]₂·3CHCl₃, [Pt(dmba)(1-Methy)(PPh₃)], [Pd(tmeda)(C₆F₅)(1-Methy)], and [NBu₄][Pd(C₆F₅)(1-Methy)₂(H₂O)]·H₂O, have been established by X-ray diffraction. Dinuclear neutral molecules of complex [Pd(dmba)(μ-1-Methy)]₂ are stacked to give centrosymmetric pairs due to intermolecular π–π interactions between 1-Methy ligands. There are also intermolecular π–π interactions between Methy ligands in [Pd(tmeda)(C₆F₅)(1-Methy)]. An interesting feature of the crystal structure of [NBu₄][Pd(C₆F₅)(1-Methy)₂(H₂O)]·H₂O is the presence of dimeric units of [Pd(C₆F₅)(H₂O)(1-Methy)₂·2H₂O] due to OH···O hydrogen bonds. The DNA adduct formation of the new platinum complexes synthesized was followed by circular dichroism and electrophoretic mobility. Atomic force microscopy images of the modifications caused by the platinum complexes on plasmid DNA pBR322 were also obtained. The changes observed are consistent with the results of electrophoretic mobility, and they confirm the strong interaction of the complexes with DNA. Values of IC₅₀ were also calculated for the new platinum complexes against the tumor cell line HL-60. All the new platinum complexes were more active than cisplatin (up to 20-fold in some cases).

Experimental Section

Instrumental Measurements. The C, H, N, and S analyses were performed with a Carlo Erba model EA 1108 microanalyzer. Decomposition temperatures were determined with a SDT 2960 simultaneous DSC-TGA of TA instruments at a heating rate of 5 °C min⁻¹ and the solid samples under nitrogen flow (100 mL min⁻¹). The ¹H, ¹³C, ³¹P, and ¹⁹F NMR spectra were recorded on a Bruker AC 200E or Bruker AC 300E spectrometer, using SiMe₄, H₃PO₄, and CFCl₃ as standards. The ¹⁹⁵Pt NMR spectra were recorded on a Bruker AV 400 spectrometer, using Na₂[PtCl₆] as standard. Infrared spectra were recorded on a Perkin-Elmer 1430 spectrophotometer using Nujol mulls between polyethylene sheets. Mass spectra (positive-ion FAB) were recorded on a V.G. Auto-SpecE spectrometer and measured using 3-nitrobenzyl alcohol as the dispersing matrix.

Materials. The starting complexes [Pd(dmba)(μ-OH)]₂,¹⁴ [Pd-(C₆F₅)(N–N)(OH)] (N–N = bpy, Me₂bpy, or tmeda),¹⁵ [Pt(dmba)-Cl(L)] (L = PPh₃ and DMSO),³³ and [Pd(C₆F₅)(NCPh)(μ-Cl)]₂⁵⁴ were prepared by procedures described elsewhere. Solvents were dried by the usual methods. 1-Methylcytosine (1-Mecyt) was purchased from Chemogen (Konstanz, Germany). 1-Methyluracil, 1-methylthymine, the sodium salt of calf thymus DNA, EDTA (ethylenediaminetetraacetic acid), and Tris-HCl (tris(hydroxymethyl)-aminomethane–hydrochloride) used in the circular dichroism (CD)

(49) Ushay, H. M.; Tullius, T. D.; Lippard, S. J. *Biochemistry* **1981**, *20*, 3744.

(50) Onoa, G. B.; Cervantes, G.; Moreno, V.; Prieto, M. J. *Nucleic Acids Res.* **1998**, *26*, 1473.

(51) Cervantes, G.; Marchal, S.; Prieto, M. J.; Pérez, J. M.; González, V. M.; Alonso, C.; Moreno, V. *J. Inorg. Biochem.* **1999**, *77*, 197.

(52) Onoa, G. B.; Moreno, V. *Int. J. Pharm.* **2002**, *245*, 55.

(53) Martin, S. J.; Green, D. R. *Curr. Opin. Oncol.* **1994**, *6*, 616.

(54) Albéniz, A. C.; Espinet, P.; Jeannin, Y.; Philoche-Levisalles, M.; Mann, B. E. *J. Am. Chem. Soc.* **1990**, *112*, 6599.

study were obtained from Sigma-Aldrich (Madrid, Spain); HEPES (*N*-(2-hydroxyethyl)piperazine-*N'*-ethanesulfonic acid) was obtained from ICN (Madrid, Spain), and pBR322 plasmid DNA was obtained from Boehringer-Mannheim (Mannheim, Germany).

Warning! Perchlorate salts of metal complexes with organic ligands are potentially explosive. Only small amounts of material should be prepared, and these should be handled with great caution.

Preparation of Complexes [Pd(dmmba)(μ -L)]₂ [L = 1-Methy (1) and 1-Meura (2)]. To a suspension of [Pd(dmmba)(μ -OH)]₂ (100 mg, 0.194 mmol) in dichloromethane (3 mL) was added 1-methylthymine or 1-methyluracil (0.388 mmol). The resulting solution was stirred at room temperature for 1 h and then concentrated under vacuum. The addition of hexane caused the precipitation of a yellow solid which was collected by filtration and air-dried.

Data for Complex 1. Yield: 65%. Anal. Calcd for C₃₀H₃₈N₆O₄Pd₂: C, 47.4; H, 5.0; N, 11.1. Found: C, 47.1; H, 5.0; N, 11.1. Mp: 197 °C (dec). IR (Nujol, cm⁻¹): 1655, 1640, 1548, 1534, 1518. ¹H NMR (CDCl₃): δ (SiMe₄) 6.78 (m, 6H, aromatics of dmmba + H(6) of 1-Methy), 6.65 (m, 2H, aromatics of dmmba), 6.31 (d, 2H, aromatics dmmba, *J* 7.7), 3.59 (d, 2H, NCH₂, *J* 13.6), 3.32 (s, 6H, NMe of 1-Methy), 3.17 (d, 2H, NCH₂, *J* 13.6), 2.94 (s, 6H, NMe₂), 1.86 (s, 6H, NMe₂), 1.77 (s, 6H, CMe of 1-Methy). ¹³C{¹H} NMR (CDCl₃): δ (SiMe₄) 139.7 (C(6) of 1-Methy), 134.0, 125.0, 123.5, 121.0 (aromatics CH dmmba), 71.6 (CH₂NMe₂), 51.9 (NMe₂), 50.6 (NMe₂), 37.1 (CH₃N of 1-Methy), 13.8 (CH₃C of 1-Methy). Positive-ion FAB mass spectrum: *m/z* 783 (M + 23)⁺, 760 (M)⁺.

Data for Complex 2. Yield: 83%. Anal. Calcd for C₂₈H₃₄N₆O₄Pd₂: C, 46.0; H, 4.7; N, 11.5. Found: C, 46.1; H, 4.8; N, 11.2. Mp: 195 °C (dec). IR (Nujol, cm⁻¹): 1640, 1542. ¹H NMR (CDCl₃): δ (SiMe₄) 6.95 (d, 2H, H(6) of 1-Meura, *J*_{H6H5} 7.3), 6.80 (m, 4H, aromatics of dmmba), 6.66 (m, 2H, aromatics of dmmba), 6.31 (d, 2H, aromatics dmmba, *J* 7.7), 5.62 (d, 2H, H(5) of 1-Meura, *J*_{H6H5} 7.3), 3.73 (d, 2H, NCH₂, *J* 13.9), 3.33 (s, 6H, NMe of 1-Meura), 3.25 (d, 2H, NCH₂, *J* 13.9), 2.96 (s, 6H, NMe₂), 2.10 (s, 6H, NMe₂). ¹³C{¹H} NMR (CDCl₃): δ (SiMe₄) 143.2 (C(6) of 1-Meura), 133.4, 125.1, 123.6, 121.1 (aromatics CH dmmba), 101.8 (C(5) of 1-Meura), 71.9 (CH₂NMe₂), 52.1 (NMe₂), 51.0 (NMe₂), 37.8 (CH₃N of 1-Meura). Positive-ion FAB mass spectrum: *m/z* 755 (M + 23)⁺, 732 (M)⁺.

Preparation of Complex [Pd(dmmba)(μ -1-Mecyt)]₂·CH₂Cl₂ (3). To a suspension of [Pd(dmmba)(μ -OH)]₂ (100 mg, 0.194 mmol) in dichloromethane (20 mL) was added 1-methylcytosine (48.5 mg, 0.388 mmol). The resulting solution was stirred under reflux for 2 h. The addition of hexane caused the precipitation of a white solid which was collected by filtration and air-dried.

Data for Complex 3. Yield: 65%. Anal. Calcd for C₂₉H₃₈N₈Cl₂O₂Pd₂: C, 42.8; H, 4.7; N, 13.8. Found: C, 42.8; H, 5.3; N, 14.1. Mp: 260 °C (dec). IR (Nujol, cm⁻¹): 3345 ν (NH), 1650, 1615, 1538. ¹H NMR (CDCl₃): δ (SiMe₄) 7.09 (dd, 2H, aromatics of dmmba, *J* 7.2, *J'* 1.5), 6.88 (m, 4H, aromatics of dmmba), 6.78 (d, 2H, aromatics dmmba, *J* 7.0), 6.55 (d, 2H, H(6) of 1-Mecyt, *J*_{H6H5} 7.2), 5.50 (d, 2H, H(5) of 1-Mecyt, *J*_{H6H5} 7.2), 5.13 (s, 2H, NH of 1-Mecyt), 3.22 (s, 6H, NMe of 1-Mecyt), 3.05 (d, 2H, NCH₂, *J* 13.8), 2.75 (s, 6H, NMe₂), 2.74 (d, 2H, NCH₂, *J* 13.8), 1.97 (s, 6H, NMe₂). ¹³C{¹H} NMR (CDCl₃): δ (SiMe₄) 138.5 (C(6) of 1-Mecyt), 133.7, 124.0, 123.3, 121.0 (aromatics CH dmmba), 100.6 (C(5) of 1-Mecyt), 71.4 (CH₂NMe₂), 52.0 (NMe₂), 50.3 (NMe₂), 36.8 (CH₃N of 1-Mecyt). Positive-ion FAB mass spectrum: *m/z* 753 (M - CH₂Cl₂ + 23)⁺, 730 (M - CH₂Cl₂)⁺.

Preparation of Complexes [Pd(dmmba)(1-Methy)(PPh₃)] (4) and [Pd(dmmba)(1-Meura)(PPh₃)]·CH₂Cl₂ (5). To a suspension of [Pd(dmmba)(μ -L)]₂ (L = 1-Methy or 1-Meura) (0.132 mmol) in dichloromethane (4 mL) was added PPh₃ (69.1 mg, 0.254 mmol).

The resulting solution was stirred at room temperature for 1 h and then concentrated under vacuum. The addition of hexane caused the precipitation of a white solid, which was collected by filtration and air-dried.

Data for Complex 4. Yield: 85%. Anal. Calcd for C₃₃H₃₄N₃O₂-PPd: C, 61.7; H, 5.3; N, 6.5. Found: C, 61.6; H, 5.5; N, 6.6. Mp: 264 °C (dec). IR (Nujol, cm⁻¹): 1660, 1640, 1570, 1545. ¹H NMR (CDCl₃): δ (SiMe₄) 7.78 (m, 6H, PPh₃), 7.33 (m, 9H, PPh₃), 6.98 (d, 1H, aromatics of dmmba, *J* 7.2), 6.81 (m, 1H, aromatics of dmmba), 6.35 (m, 2H, aromatics dmmba), 6.28 (d, 1H, H(6) of MeT, *J*_{HP} 1.2), 4.15 (dd, 1H, NCH₂, *J*_{HH} 13.6, *J*_{HP} 1.5), 3.98 (dd, 1H, NCH₂, *J*_{HH} 13.6, *J*_{HP} 2.2), 2.93 (s, 3H, NMe of 1-Methy), 2.80 (d, 3H, NMe₂, *J*_{HP} 2.3), 2.77 (d, 3H, NMe₂, *J*_{HP} 2.5), 1.57 (d, 3H, CMe of 1-Methy, *J*_{HP} 1.0). ¹³C{¹H} NMR (CDCl₃): δ (SiMe₄) 138.7 (C(6) of 1-Methy and aromatic CH dmmba), 135.1, 130.2, 127.7 (aromatics CH PPh₃), 124.4, 123.4, 121.9 (aromatics CH dmmba), 72.6 (CH₂NMe₂), 51.1 (NMe₂), 36.3 (NCH₃ of 1-Methy), 13.7 (CH₃C of 1-Methy). ³¹P NMR (CDCl₃): δ (H₃PO₄) 44.0 (s). Positive-ion FAB mass spectrum: *m/z* 643 (M + 1)⁺.

Data for Complex 5. Yield: 80%. Anal. Calcd for C₃₃H₃₄N₃Cl₂O₂PPd: C, 55.6; H, 4.8; N, 5.8. Found: C, 55.4; H, 4.8; N, 5.9. Mp: 248 °C (dec). IR (Nujol, cm⁻¹): 1640, 1564, 1548. ¹H NMR (CDCl₃): δ (SiMe₄) 7.80 (m, 6H, PPh₃), 7.30 (m, 9H, PPh₃), 6.99 (d, 1H, aromatic dmmba, *J* 7.2), 6.82 (m, 1H, aromatic of dmmba), 6.47 (d, 1H, H(6) of 1-Meura, *J*_{H6H5} 7.2), 6.35 (m, 2H, aromatics of dmmba), 5.14 (d, 1H, H(5) of 1-Meura, *J*_{H6H5} 7.2), 4.17 (dd, 1H, NCH₂, *J*_{HH} 13.6, *J*_{HP} 2.1), 3.97 (dd, 1H, NCH₂, *J*_{HH} 13.6, *J*_{HP} 2.4), 2.90 (s, 3H, NMe of 1-Meura), 2.78 (d, 3H, NMe₂, *J*_{HP} 2.1), 2.76 (d, 3H, NMe₂, *J*_{HP} 2.4). ¹³C{¹H} NMR (CDCl₃): δ (SiMe₄) 142.4 (C(6) of 1-Meura), 138.5 (aromatic CH dmmba), 135.1, 130.2, 127.9 (aromatics CH PPh₃), 124.4, 123.4, 121.9 (aromatics CH dmmba), 102.3 (C(5) of 1-Meura), 72.6 (CH₂NMe₂), 50.6 (NMe₂), 50.4 (NMe₂), 36.5 (NCH₃ of 1-Meura). ³¹P NMR (CDCl₃): δ (H₃PO₄) 41.8 (s). Positive-ion FAB mass spectrum: *m/z* 702 (M - Meura)⁺.

Preparation of Complexes [Pt(dmmba)(1-Methy)(L')]₂ (6, 8) and [Pt(dmmba)(1-Meura)(L')]₂ (7, 9). To a solution of [Pt(dmmba)(Cl)(L')]₂ (L' = PPh₃ or DMSO) (0.159 mmol) in acetone (20 mL) was added AgClO₄ (33.0 mg, 0.159 mmol). AgCl immediately formed. The resulting suspension was stirred for 30 min and then filtered through a short pad of Celite. To the filtrate was then added 20% [NBu₄]OH(aq) (209 μ L, 0.159 mmol) and finally either 1-MethyH or 1-MeuraH (0.159 mmol). The resulting solution was stirred at room temperature for 6 h and then concentrated under vacuum. The resulting white precipitate was collected by filtration and air-dried.

Data for Complex 6. Yield: 82%. Anal. Calcd for C₃₃H₃₄N₃O₂-PPt: C, 54.2; H, 4.7; N, 5.8. Found: C, 54.1; H, 4.9; N, 5.6. Mp: 303 °C (dec). IR (Nujol, cm⁻¹): 1660, 1640, 1580. ¹H NMR (CDCl₃): δ (SiMe₄) 7.80 (m, 6H, PPh₃), 7.33 (m, 9H, PPh₃), 7.02 (d, 1H, aromatics of dmmba, *J* 7.2), 6.82 (m, 1H, aromatics of dmmba), 6.48 (m, 2H, aromatics dmmba), 6.30 (d, 1H, H(6) of 1-Methy, *J*_{HP} 1.0), 4.13 (dd, 1H, NCH₂, *J*_{HH} 13.6, *J*_{HP} 2.1), 3.99 (dd, 1H, NCH₂, *J*_{HH} 13.6, *J*_{HP} 3.0), 2.94 (s, 3H, NMe of 1-Methy), 2.91 (d, 3H, NMe₂, *J*_{HP} 2.7), 2.88 (d, 3H, NMe₂, *J*_{HP} 2.7), 1.57 (s, 3H, CMe of 1-Methy, *J*_{HP} 0.6). ¹³C{¹H} NMR (CDCl₃): δ (SiMe₄) 140.3 (C(6) of 1-Methy), 140.2 (d, aromatic CH dmmba, *J*_{HP} 6.2), 137.2, 132.0, 129.4 (aromatics CH PPh₃), 126.5, 124.4, 123.2 (aromatics CH dmmba), 75.3 (CH₂NMe₂), 52.8 (NMe₂), 38.2 (NCH₃ of 1-Methy), 15.4 (CH₃C of 1-Methy). ³¹P NMR (CDCl₃): δ (H₃PO₄) 21.2 (s, *J*_{Pt-P} 4412). ¹⁹⁵Pt NMR (CDCl₃): δ (Na₂[PtCl₆]) -4013 (d, *J*_{Pt-P} 4412). Positive-ion FAB mass spectrum: *m/z* 730 (M)⁺.

Data for Complex 7. Yield: 87%. Anal. Calcd for C₃₂H₃₂N₃O₂-PPt: C, 53.6; H, 4.5; N, 5.9. Found: C, 53.8; H, 4.7; N, 5.9. Mp:

288 °C (dec). IR (Nujol, cm^{-1}): 1643, 1568. ^1H NMR (CDCl_3): $\delta(\text{SiMe}_4)$ 7.80 (m, 6H, PPh_3), 7.30 (m, 9H, PPh_3), 7.02 (d, 1H, aromatic dmba, J 7.2), 6.82 (m, 1H, aromatic of dmba), 6.50 (m, 3H, H(6) of 1-Meura + 2 H of aromatics of dmba), 5.18 (d, 1H, H(5) of 1-Meura, J_{H6H5} 7.3), 4.14 (dd, 1H, NCH_2 , J_{HH} 13.2, J_{HP} 2.0), 4.00 (dd, 1H, NCH_2 , J_{HH} 13.2, J_{HP} 2.8), 2.91 (s, 3H, NMe_2 of dmba), 2.88 (d, 3H, NMe_2 of dmba, J_{HP} 2.5), 2.16 (s, 3H, NMe_2 of 1-Meura). $^{13}\text{C}\{^1\text{H}\}$ NMR (CDCl_3): $\delta(\text{SiMe}_4)$ 142.4 (C(6) of 1-Meura), 138.6 (d, aromatic CH dmba, J_{HP} 6.2), 135.5, 130.5, 128.1 (aromatics CH PPh_3), 125.1, 123.0, 123.0 (aromatics CH dmba), 102.9 (C(5) of 1-Meura), 73.8 (CH_2NMe_2 , J_{HP} 3.1), 51.3 (NMe_2 , J_{HP} 13.6), 37.2 (NMe_2), 31.4 (NCH_3 of 1-Meura). ^{31}P NMR (CDCl_3): $\delta(\text{H}_3\text{PO}_4)$ 20.9 (s, $J_{\text{Pt-P}}$ 4403). ^{195}Pt NMR (CDCl_3): $\delta(\text{Na}_2[\text{PtCl}_6])$ -4013 (d, $J_{\text{Pt-P}}$ 4403). Positive-ion FAB mass spectrum: m/z 716 (M^+).

Data for Complex 8. Yield: 86%. Anal. Calcd for $\text{C}_{17}\text{H}_{25}\text{N}_3\text{O}_3\text{-SPT}$: C, 37.4; H, 4.6; N, 7.7; S, 5.9. Found: C, 37.7; H, 4.5; N, 7.5; S, 5.7. Mp: 237 °C (dec). IR (Nujol, cm^{-1}): 1668, 1658, 1644, 1574. ^1H NMR (CDCl_3): $\delta(\text{SiMe}_4)$ 7.93 (d, 1H, aromatics of dmba, J 7.9, J_{HPt} 38.0), 7.05 (m, 3H, aromatics of dmba), 6.93 (s, 1H, H(6) of 1-Methy), 4.01 (d, 1H, NCH_2 , J_{HH} 13.1), 3.92 (d, 1H, NCH_2 , J_{HH} 13.1), 3.31 (s, 3H, NMe of 1-Methy), 3.27 (s, 3H, DMSO, J_{HPt} 30.0), 3.18 (s, 3H, DMSO, J_{HPt} 25.5), 2.72 (s, 3 H, NMe_2 , J_{HPt} 34.6), 2.70 (s, 3 H, NMe_2 , J_{HPt} 33.0), 1.86 (s, 3H, CMe of 1-Methy). $^{13}\text{C}\{^1\text{H}\}$ NMR (CDCl_3): δ 140.4 (C(6) of 1-Methy), 135.2, 126.3, 124.8, 122.0, (aromatics CH dmba), 75.0 (CH_2NMe_2), 52.0 (NMe_2), 51.9 (NMe_2), 47.0 (DMSO), 46.4 (DMSO), 37.1 (NCH_3 of 1-Methy), 13.9 (CH_3C of 1-Methy). ^{195}Pt NMR (CDCl_3): $\delta(\text{Na}_2[\text{PtCl}_6])$ -3673. Positive-ion FAB mass spectrum: m/z 546 (M^+).

Data for Complex 9. Yield: 78%. Anal. Calcd for $\text{C}_{16}\text{H}_{23}\text{N}_3\text{O}_3\text{-SPT}$: C, 36.1; H, 4.4; N, 7.9; S, 6.0. Found: C, 35.8; H, 4.1; N, 7.7; S, 5.7. Mp: 238 °C (dec). IR (Nujol, cm^{-1}): 1640, 1574. ^1H NMR (CDCl_3): $\delta(\text{SiMe}_4)$ 7.95 (d, 1 H, aromatic dmba, J 7.2, J_{HPt} 37.6), 7.11 (m, 4 H, aromatic of dmba + H(6) of 1-Meura), 5.66 (d, 1H, H(5) of 1-Meura, J_{H6H5} 7.5), 4.02 (d, 1H, NCH_2 , J_{HH} 13.1), 3.96 (d, 1H, NCH_2 , J_{HH} 13.1), 3.36 (s, 3H, NMe of 1-Meura), 3.29 (s, 3H, DMSO, J_{HPt} 25.5), 3.20 (s, 3H, DMSO, J_{HPt} 26.0), 2.72 (s, 6 H, NMe_2 , J_{PH} 30.8). $^{13}\text{C}\{^1\text{H}\}$ NMR (CDCl_3): $\delta(\text{SiMe}_4)$ 145.4 (C(6) of 1-Meura), 136.7, 127.8, 126.3, 123.5 (aromatics CH dmba), 104.9 (C(5) of 1-Meura), 76.4 (CH_2NMe_2), 53.5 (NMe_2), 53.4 (NMe_2), 48.4 (DMSO), 47.9 (DMSO), 38.9 (NCH_3 of 1-Meura). ^{195}Pt NMR (CDCl_3): $\delta(\text{Na}_2[\text{PtCl}_6])$ -3674. Positive-ion FAB mass spectrum: m/z 702 ($\text{M} + 1^+$).

Preparation of Complexes [Pd(N-N)(C₆F₅)(L)] (N-N = bpy or Me₂bpy) (10, 11). To a solution of the corresponding hydroxo complex [Pd(N-N)(C₆F₅)(OH)] (0.243 mmol) in acetone (15 mL) was added 1-MethyH or 1-MeuraH (0.243 mmol). The resulting mixture was stirred for 12 h at room temperature to yield a white suspension. The precipitate was filtered off and air-dried.

Data for Complex 10. Yield: 73%. Anal. Calcd for $\text{C}_{22}\text{H}_{15}\text{F}_5\text{N}_4\text{-O}_2\text{Pd}$: C, 46.5; H, 2.7; N, 9.9. Found: C, 46.6; H, 2.5; N, 9.7. Mp: 281 °C (dec). IR (Nujol, cm^{-1}): 1690, 1682, 1660, $\nu(\text{Pd}-\text{C}_6\text{F}_5)$, 780. ^1H NMR (CDCl_3): $\delta(\text{SiMe}_4)$ 8.13 (m, 3H, bpy), 7.93 (m, 3H, bpy), 7.28 (m, 2H, $\text{H}_\beta + \text{H}_\beta$), 6.80 (s, 1H, H(6) of 1-Methy), 3.31 (s, 3H, NMe of 1-Methy), 1.82 (s, 3H, CMe of 1-Methy). ^{19}F NMR (CDCl_3): $\delta(\text{CFCl}_3)$ -117.9 (m, 1F_o), -118.7 (m, 1F_o), -160.9 (t, 1F_p , $J(\text{F}_m\text{F}_p)$ 21.0 Hz), -163.0 (m, 2F_m). Positive-ion FAB mass spectrum: m/z 569 ($\text{M} + 1^+$).

Data for Complex 11. Yield: 65%. Anal. Calcd for $\text{C}_{23}\text{H}_{17}\text{F}_5\text{N}_4\text{-O}_2\text{Pd}$: C, 47.4; H, 2.9; N, 9.6. Found: C, 47.1; H, 2.9; N, 9.7. Mp: 284 °C (dec). IR (Nujol, cm^{-1}): 1650, 1644, 1620, 1580, $\nu(\text{Pd}-\text{C}_6\text{F}_5)$, 790. ^1H NMR (CDCl_3): $\delta(\text{SiMe}_4)$ 7.95 (d, H_α , $J(\text{H}_\alpha\text{H}_\beta)$ 6.0), 7.86 (s, 2H, $\text{H}_\delta + \text{H}_\delta$), 7.70 (d, H_α , $J(\text{H}_\alpha\text{H}_\beta)$ 6.0),

7.16 (d, 1H, H_β , $J(\text{H}_\alpha\text{H}_\beta)$ 6.0), 7.01 (d, 1H, H_β , $J(\text{H}_\alpha\text{H}_\beta)$ 6.0), 6.90 (d, 1H, H(6) of 1-Meura, J_{H6H5} 7.3), 5.5 (d, 1H, H(5) of 1-Meura, J_{H6H5} 7.3), 3.30 (s, 3H, NMe of 1-Meura), 2.4 (s, 6H, Me of Me₂bpy). ^{19}F NMR (CDCl_3): $\delta(\text{CFCl}_3)$ -118.9 (d, 1F_o , $J(\text{F}_o\text{F}_m)$ 32.2), -118.5 (d, 1F_o , $J(\text{F}_o\text{F}_m)$ 39.2), -161.1 (t, 1F_p , $J(\text{F}_m\text{F}_p)$ 31.0), -163.3 (m, 2F_m). Positive-ion FAB mass spectrum: m/z 583 ($\text{M} + 1^+$).

Preparation of Complexes [Pd(tmeda)(C₆F₅)(L)] (12, 13). To a solution of the hydroxo complex [Pd(tmeda)(C₆F₅)(OH)] (100 mg, 0.246 mmol) in acetone (15 mL) was added 1-MethyH or 1-MeuraH (0.246 mmol). The resulting mixture was stirred for 12 h at room temperature. The solvent was partially evaporated under reduced pressure. On addition of hexane, the complexes **12** and **13** precipitated and were filtered off and air-dried.

Data for Complex 12. Yield: 68%. Anal. Calcd for $\text{C}_{18}\text{H}_{23}\text{F}_5\text{N}_4\text{-O}_2\text{Pd}$: C, 40.9; H, 4.4; N, 10.6. Found: C, 41.2; H, 4.4; N, 10.3. Mp: 285 °C (dec). IR (Nujol, cm^{-1}): 1678, 1664, 1642, 1586, $\nu(\text{Pd}-\text{C}_6\text{F}_5)$, 780. ^1H NMR (CDCl_3): $\delta(\text{SiMe}_4)$ 6.85 (s, 1H, H(6) of 1-Methy), 3.10 (s, 3H, NMe of 1-Methy), 2.90 (m, 4H, CH_2), 2.61 (s, 3H, Me), 2.60 (s, 3H, Me), 2.58 (s, 3H, Me), 2.56 (s, 3H, Me), 1.64 (s, 3H, CMe of 1-Methy). ^{19}F NMR (CDCl_3): $\delta(\text{CFCl}_3)$ -114.9 (m, 1F_o), -115.5 (m, 1F_o), -164.6 (t, 1F_p , $J(\text{F}_m\text{F}_p)$ 20.7 Hz), -166.6 (m, 2F_m). Positive-ion FAB mass spectrum: m/z 529 ($\text{M} + 1^+$).

Data for Complex 13. Yield: 69%. Anal. Calcd for $\text{C}_{17}\text{H}_{21}\text{F}_5\text{N}_4\text{-O}_2\text{Pd}$: C, 39.7; H, 4.1; N, 10.9. Found: C, 39.9; H, 4.1; N, 10.7. Mp: 208 °C (dec). IR (Nujol, cm^{-1}): 1660, 1650, 1644, 1580, $\nu(\text{Pd}-\text{C}_6\text{F}_5)$, 784. ^1H NMR (CDCl_3): $\delta(\text{SiMe}_4)$ 7.01 (d, 1H, H(6) of 1-Meura, J_{H6H5} 7.2), 5.10 (d, 1H, H(5) of 1-Meura, J_{H6H5} 7.2), 3.12 (s, 3H, NMe of 1-Meura), 2.90 (m, 4H, CH_2), 2.61 (s, 6H, Me), 2.60 (s, 3H, Me), 2.58 (s, 3H, Me). ^{19}F NMR (CDCl_3): $\delta(\text{CFCl}_3)$ -113.7 (m, 1F_o), -114.2 (m, 1F_o), -163.4 (t, 1F_p , $J(\text{F}_m\text{F}_p)$ 20.7 Hz), -165.4 (m, 2F_m). Positive-ion FAB mass spectrum: m/z 515 ($\text{M} + 1^+$).

Preparation of Complex [NBu₄][Pd(C₆F₅)(1-Methy)₂(OH)₂] (14). To a solution of 1-methylthymine (68 mg, 0.485 mmol) in acetone (5 mL) was added 20% [NBu₄]OH(aq) (636 μL , 0.485 mmol). To the resulting solution was added a solution of [Pd(C₆F₅)(NCPH)(μ -Cl)₂] (100 mg, 0.121 mmol) in acetone (15 mL). The mixture was stirred at room temperature for 24 h and then filtered through a short pad of Celite. Solvent was partially evaporated under reduced pressure. On addition of water the yellow complex **14** precipitated and was filtered off and air-dried.

Data for Complex 14. Yield: 50%. Anal. Calcd for $\text{C}_{34}\text{H}_{52}\text{F}_5\text{N}_5\text{-O}_3\text{Pd}$: C, 50.3; H, 6.5; N, 8.6. Found: C, 50.1; H, 6.7; N, 8.3. Mp: 202 °C (dec). IR (Nujol, cm^{-1}): 1667, 1631, 1575, $\nu(\text{Pd}-\text{C}_6\text{F}_5)$, 776. ^1H NMR (acetone-*d*₆): $\delta(\text{SiMe}_4)$ 7.03 (2H, H(6) of 1-Methy), 3.1 (s, 6 H, NMe of 1-Methy), 1.70 (s, 6H, CMe of 1-Methy). ^{19}F NMR (acetone-*d*₆): $\delta(\text{CFCl}_3)$ -116.3 (m, 2F_o , $J(\text{F}_o\text{F}_m)$ 28.2 Hz), -168.0 (t, 1F_p , $J(\text{F}_m\text{F}_p)$ 19.8 Hz), -169.7 (m, 2F_m). Positive-ion FAB mass spectrum: m/z 552 ($\text{M} + 1 - \text{H}_2\text{O}^+$).

Reactions of the Platinum Complex 8 with 9-Ethylguanine and Guanosine. Both reactions were carried out in NMR tubes (D₂O and 5% DMSO-*d*₆ as solvents). 9-Ethylguanine or guanosine was incubated with complex **8** in a ratio 5:1 in D₂O at pH 7.0 (50 mM KD₂PO₄) and 37 °C. The concentration of complex **8** was 5.0 mM. Both reactions were very fast, and in less than 5 min the formation of the corresponding complex [Pt(dmba)(DMSO)(L)]⁺ (L = 9-EtG or guanosine) was completed.

^1H NMR data for the reaction of **8** with 9-ethylguanine: $\delta(\text{SiMe}_4)$ 8.66 (s, 1H, H(8) of coordinated EtG), 7.89 (s, H(8) of free guanosine in excess), 7.76 (d, 1H, aromatics of dmba, J 7.5), 7.50 (s, 1H, H(6) of free 1-Methy), 7.29 (m, 3H, aromatics of dmba),

Table 11. Crystal Structure Determination Details

param	1	3·2CHCl ₃	4·3CHCl ₃	6	12	14·H ₂ O
empirical formula	C ₃₀ H ₃₈ N ₆ O ₄ Pd ₂	C ₂₈ H ₃₆ N ₈ O ₂ Pd ₂ ·2CHCl ₃	C ₂₄ H _{24.67} Cl ₆ N ₂ O _{1.33} P _{0.67} Pd _{0.67}	C ₃₃ H ₃₄ N ₃ O ₂ Pt	C ₁₈ H ₂₃ F ₅ N ₄ O ₂ Pd	C ₃₄ H ₅₄ F ₅ N ₅ O ₆ Pd
fw	759.46	968.18	666.74	730.69	528.80	830.22
cryst system	monoclinic	monoclinic	triclinic	monoclinic	monoclinic	monoclinic
<i>a</i> (Å)	9.9003(2)	20.1123(11)	10.1410(10)	18.2589(11)	21.686(2)	15.419(1)
<i>c</i> (Å)	19.3077(4)	9.7760(11)	14.6570(10)	8.0212(5)	19.712(2)	16.771(1)
<i>c</i> (Å)	16.9681(4)	20.7128(11)	16.1070(10)	20.8978(13)	11.9190(10)	15.510(1)
α (deg)	90	90	80.220(10)	90	90	90
β (deg)	106.19	92.273(5)	72.170(10)	106.368(2)	108.457(7)	97.43(1)
γ (deg)	90	90	73.140(10)	90	90	90
<i>V</i> (Å ³)	3114.81(12)	4069.3(6)	2172.5(3)	2936.6(3)	4833.0(8)	3977.1(5)
temp (K)	293(2)	173(2)	173(2)	100(2)	293(2)	293(2)
space group	<i>P</i> 2 ₁ / <i>n</i>	<i>P</i> 2 ₁ / <i>n</i>	<i>P</i> 1	<i>P</i> 2 ₁ / <i>c</i>	<i>C</i> 2/ <i>c</i>	<i>P</i> 2 ₁ / <i>n</i>
<i>Z</i>	4	4	2	4	8	4
μ (mm ⁻¹)	1.199	1.315	1.053	4.867	0.825	0.537
reflcs colld	21 088	10 388	8512	31 104	5650	13 970
indpdnt reflns	7737	7164	7571	5977	4267	6990
R(int)	0.0305	0.0368	0.0255	0.0451	0.0115	0.0328
R1 [<i>I</i> > 2σ(<i>I</i>)] ^a	0.0328	0.0376	0.0763	0.0266	0.0411	0.0487
wR2 (all data) ^b	0.0829	0.0936	0.2318	0.0580	0.1511	0.1284

^a R1 = Σ||*F*_o| - |*F*_c||/Σ|*F*_o|, wR2 = [Σ[w(*F*_o² - *F*_c²)²]/Σw(*F*_o²)]^{0.5}. ^b w = 1/[σ(*F*_o²) + (*aP*)² + *bP*], where *P* = (2*F*_c² + *F*_o²)/3 and *a* and *b* are constants set by the program.

4.28 (q, 4H, CH₂ of coordinated EtG, *J* 7.2), 4.14 (q, CH₂ of free EtG in excess, *J* 7.2), 3.41 (s, 3H, DMSO, *J*_{HPt} 19.5), 3.39 (s, 3H, *NMe* of free 1-Methy), 3.16 (s, 3H, DMSO, *J*_{HPt} 21.6), 2.66 (s, 3H, *NMe*₂, *J*_{HPt} 34.0), 2.51 (s, 3H, *NMe*₂, *J*_{HPt} 35.9), 1.93 (s, 3H, *CMe* of free 1-Methy), 1.56 (t, 3H, Me of coordinated EtG, *J* 7.2), 1.47 (t, 3H, Me of free EtG in excess, *J* 7.2).

¹H NMR data for the reaction of **8** with guanosine: δ(SiMe₄) 8.86 (s, 1H, H(8) of coordinated guanosine), 8.05 (s, H(8) of free guanosine in excess), 7.75 (d, 1H, aromatics of dmbs, *J* 7.2), 7.51 (s, 1H, H(6) of free 1-Methy), 7.32 (m, 3H, aromatics of dmbs), 6.08 (d, 1H, H(1)' of coordinated guanosine, *J* 5.1), 5.96 (d, H(1)' of free guanosine in excess, *J* 6.0).

Reaction of the Platinum Complex 6 with 9-Ethylguanine. The reaction was carried out in a NMR tube (D₂O and 5% DMSO-*d*₆ as solvents). 9-Ethylguanine was incubated with **6** in a ratio 5:1 in D₂O at pH 7.0 (50 mM KD₂PO₄) and 37 °C. The reaction was very fast, and in less than 5 min the formation of the complex [Pt(dmbs)(PPh₃)(9-EtG)]⁺ was completed.

¹H NMR data for the reaction of **6** with 9-ethylguanine: δ(SiMe₄) 8.24 (s, 1H, H(8) of coordinated EtG), 7.90 (s, H(8) of free EtG in excess), 7.81 (m, 6H, PPh₃), 7.63 (m, 3H, PPh₃), 7.55 (s, H(6) of free 1-Methy), 7.42 (m, 6H, PPh₃), 7.28 (d, 1H, aromatics of dmbs, *J* 8.0), 7.04 (m, 1H, aromatics of dmbs), 6.61 (m, 1H, aromatics of dmbs), 6.53 (d, 1H, aromatics of dmbs, *J* 7.5), 4.28 (q, CH₂ of free EtG, *J* 7.2), 3.39 (s, *NMe* of free 1-Methy), 1.93 (s, *CMe* of free 1-Methy), 1.47 (t, 3H, Me of free EtG in excess, *J* 7.2). Unfortunately, the aliphatic signals of the coordinated ligands of the new complex were obscured by those of the solvents or free ligands in excess, in part due to the low solubility of this new compound.

X-ray Crystal Structure Analysis. Suitable crystals of **1**, **3**·2CHCl₃, and **4**·3CHCl₃ were grown from chloroform/hexane. Crystals from **6**, **12**, and **14**·H₂O were grown from acetone/hexane. The crystal and molecular structures of the compounds **1**, **3**·2CHCl₃, **4**·3CHCl₃, **6**, **12**, and **14**·H₂O have been determined by X-ray diffraction studies (Table 11).

The crystals were mounted onto the tip of a glass fiber, and the data collection was performed with a Siemens P4 diffractometer for complexes **1**, **3**·2CHCl₃, **4**·3CHCl₃, and **12**, and with a Bruker Smart CCD diffractometer for complexes **6** and **14**·H₂O. The structures were solved by heavy atom and direct methods SHELXS-

97⁵⁵ and refined anisotropically on *F*².⁵² Hydrogen atoms were included using a riding model, except for those of the methyl groups in complex **6** for which a rigid model was used.

Biological Assays. Formation of Compound–DNA Complexes. The platinum compounds **6**–**9** were dissolved in DMSO prior to dilution with saline. The final maximum DMSO concentration in the growth medium was 2%. Stock solutions of each compound (1 mg/mL) were stored in the dark at room temperature until use. Compound–DNA complex formation was accomplished by addition of CT DNA (calf thymus DNA) to aliquots of each of the compounds at different concentrations in TE buffer (50 mM NaCl, 10 mM Tris-HCl, 0.1 mM EDTA, pH 7.4). The amount of compound added to the DNA solution was designated as *r*₁ (the input molar ratio of Pt or ligand to nucleotide). The mixture was incubated at 37 °C for 24 h.

Circular Dichroism Study. The CD spectra of the complex–DNA compounds (DNA concentration 20 μg/mL, *r*₁ = 0.10, 0.30, and 0.50) were recorded at room temperature on a Applied Photophysics Π*-180 spectrometer with a 75 W xenon lamp using a computer for spectral subtraction and smooth reduction. Each sample was scanned twice in a range of wavelengths between 220 and 330 nm. The drawn CD spectra are the means of two independent scans. The data are expressed as mean residue molecular ellipticity [θ] in deg cm² dmol⁻¹. The CD spectra of the complexes were subtracted from the CD spectra of each of the complex–DNA adducts by computer.

Electrophoretic Mobility Study. pBR322 DNA aliquots (0.25 μg/mL) were incubated in the presence of compounds in TE buffer at the molar ratio *r*₁ = 0.50 for electrophoresis studies. Incubation was carried out in the dark at 37 °C for 24 h; 24 μL aliquots of complex–DNA compounds containing 0.7 μg DNA underwent 1% agarose gel electrophoresis for 5 h at 1.5 V/cm in 1XTBE (45 mM Tris-borate, 1 mM EDTA pH 8.0) buffer. Gel was subsequently stained in the same buffer containing ethidium bromide (1 μg/mL). The DNA bands were visualized under UV light and photographed with a digital camera.

Atomic Force Microscopy. Preparation of Adducts DNA–Metal Complexes. pBR322 DNA (25 μg/μL) was incubated in an appropriate volume with the required platinum concentration

(55) Sheldrick, G. M. *SHELXL-97; Programs for Crystal Structure Analysis*, release 97-2; University of Göttingen: Göttingen, Germany, 1998.

corresponding to the molar ratio $r_1 = 0.005$. The complexes were dissolved in HEPES buffer (40 mM HEPES, pH 7.4, and 10 mM MgCl_2). The different solutions as well as Milli-Q water were passed through 0.2 nm FP030/3 filters (Schleicher & Schuell GmbH, Germany) and centrifuged at 4000g several times to avoid salt deposits and provide a clear background when they were imaged by AFM. The reactions were run at 37 °C for 24 h in the dark.

Sample Preparation for Atomic Force Microscopy. Samples were prepared by placing a drop (3 μL) of DNA solution or DNA–metal complex solution onto green mica (Ashville-Schoonmaker Mica Co., Newport News, VA). After adsorption for 5 min at room temperature, the samples were rinsed for 10 s in a jet of deionized water of 18 $\text{M}\Omega\text{ cm}^{-1}$ from a Milli-Q water purification system directed onto the surface with a squeeze bottle. They were then placed into an ethanol–water mixture (1:1) five times and plunged three times each in 100% ethanol. The samples were blow dried with compressed argon over silica gel and then imaged in the AFM.

Imaging by Atomic Force Microscopy. The samples were imaged in a Nanoscope III Multimode AFM (Digital Instrumentals Inc., Santa Barbara, CA) operating in tapping mode in air at a scan rate of 1–3 Hz. The AFM probe was a 125-mm-long monocrystalline silicon cantilever with integrated conical-shaped Si tips (Nanosensors GmbH, Germany) with an average resonance frequency $f_0 = 330\text{ kHz}$ and spring constant $K = 50\text{ N/m}$. The cantilever is rectangular, and the tip radius given by the supplier is 10 nm with a cone angle of 35° and high aspect ratio. In general, the images were obtained at room temperature ($T = 23 \pm 2\text{ }^\circ\text{C}$) and the relative humidity (RH) was typically lower than 40%.

Cell Line and Culture. The cell line used in this experiment was the human acute promyelocytic leukemia cell line HL-60 (American Type Culture Collection (ATCC)). Cells were routinely maintained in RPMI-1640 medium supplemented with 10% (v/v) heat-inactivated fetal bovine serum, 2 mmol/L glutamine, 100 U/mL penicillin, and 100 $\mu\text{g/mL}$ streptomycin (Life Technologies, Inc.) in a highly humidified atmosphere of 95% air with 5% CO_2 at 37 °C.

Cytotoxicity Assay. Growth inhibitory effect of platinum complexes on the leukemia HL-60 cell line was measured by the microculture tetrazolium [3-(4,5-dimethylthiazol-2-yl)-2,5-diphenyl-tetrazolium bromide, MTT] assay.⁵⁶ Briefly, cells growing in the

logarithmic phase were seeded into 96-well microtiter plates in 100 μL of the appropriate culture medium at plating density of 1×10^4 cells/well. Following the addition of different complex concentrations to quadruplicate wells, plates were incubated at 37 °C for 24 or 72 h. Aliquots of 20 μL of MTT solution were then added to each well. After 3 h, the color formed was quantified by a spectrophotometric plate reader (Bio-Tek Instruments, Inc.) at 490 nm wavelength. The percentage cell viability was calculated by dividing the average absorbance of the cells treated with a palladium or platinum complex by that of the control; % cell viability vs drug concentration (logarithmic scale) was plotted to determine the IC_{50} (drug concentration at which 50% of the cells are viable relative to the control), with its estimated error derived from the average of 3 trials.

In Vitro Apoptosis Assay. Induction of apoptosis in vitro by the platinum complexes **6–9** and cisplatin was determined by a flow cytometric assay with Annexin V-FITC⁵⁷ by using an Annexin V-FITC apoptosis detection kit (Roche). Exponentially growing HL-60 cells in 6-well plates (5×10^5 cells/well) were exposed to IC_{50} concentrations of cisplatin or complexes **6–9** for 24 h. Then the cells were subjected to staining with the Annexin V-FITC and propidium iodide as detailed by the manufacturer. The amount of apoptotic cells was analyzed by flow cytometry (BD FACSCalibur).

Acknowledgment. This work was supported by the Dirección General de Investigación del Ministerio de Ciencia y Tecnología (Project No. CTQ2005-09231-C02-01/BQU and BIO2004-05879) of Spain and the Fundación Séneca de la Comunidad Autónoma de la Región de Murcia (Project No. 00448/PI/04). We thank Dr. María José Prieto (AFM), Dr. Francisca García (Cell Culture Facility), and Manuela Costa (Cytometry Facility) for technical assistance.

Supporting Information Available: X-ray crystallography data for the complexes **1**, **3**·2 CHCl_3 , **4**·3 CHCl_3 , **6**, **12**, and **14**· H_2O and complementary figures corresponding to the NMR spectroscopic studies of the reactions of complex **8** with 9-ethylguanine and guanosine. This material is available free of charge via the Internet at <http://pubs.acs.org>.

IC060374E

(56) Mosmann, T. *J. Immunol. Methods* **1983**, *65*, 55.

(57) Vermees I, Haanen C, Steffens-Nakken H, Reutelingsperger, C. *J. Immunol. Methods* **1995**, *184*, 39.